

Florida State University Libraries

2018

Assessment of High-Resolution Regional Ocean Prediction Systems Using Multi-Platform Observations: Illustrations in the Western Mediterranean Sea

Baptiste Mourre, Eva Aguiar, Melanie Juza, Jaime Hernandez-Lasheras, Emma Reyes, Emma Heslop, Romain Escudier, Eugenio Cutolo, Simon Ruiz, Evan Mason, Ananda Pascual and Joaquin Tintore

Terms and Conditions: Readers may view, browse, and/or download material for temporary copying purposes only, provided these uses are for noncommercial personal purposes. Except as provided by law, this material may not be further reproduced, distributed, transmitted, modified, adapted, performed, displayed, published, or sold in whole or in part, without prior written permission from GODAE OceanView.



Assessment of High-Resolution Regional Ocean Prediction Systems Using Multi-Platform Observations: Illustrations in the Western Mediterranean Sea

Baptiste Mourre¹, Eva Aguiar¹, Mélanie Juza¹, Jaime Hernandez-Lasheras¹, Emma Reyes¹, Emma Heslop³, Romain Escudier⁴, Eugenio Cutolo¹, Simon Ruiz², Evan Mason², Ananda Pascual², and Joaquin Tintoré^{1,2}

¹SOCIB, Balearic Islands Coastal Observing and Forecasting System, Palma, Spain; ²IMEDEA, UIB-CSIC, Esporles, Spain; ³IOC-UNESCO, Paris, France; ⁴Department of Environmental Sciences, Rutgers, The State University of New Jersey, USA

High-resolution regional models of the ocean circulation are now operated on a routine basis using realistic setups in many regions of the world, with the aim to be used for both scientific purposes and practical applications involving decision-making processes. While the evaluation of these simulations is essential for the provision of reliable information to users and allows the identification of areas of model improvement, it also highlights several challenges. Observations are limited and the real state of the ocean is, to a large extent, unknown at the short spatiotemporal scales resolved in these models. The skill of the model also generally varies with the region, variable, depth and the spatiotemporal scale under consideration. Moreover, the increased spatial resolution might require ad hoc metrics to properly reflect the model performance and reduce the impact of so-called “double-penalty” effects occurring when using point-to-point comparisons with features present in the model but misplaced with respect to the observations. Multi-platform observations currently collected through regional and coastal ocean observatories constitute very valuable databases to evaluate the simulations. Gliders, high frequency radars, moorings, Lagrangian surface drifters, and profiling floats all provide, with their own specific sampling capability, partial but accurate information about the ocean and its variability at different scales. This is complementary to the global measurements collected from satellites. Using a case study in the Western Mediterranean Sea, this chapter illustrates the opportunities offered by multi-platform measurements to assess the realism of high-resolution regional model simulations.

Introduction

The development of operational oceanography has enabled the production of high-resolution regional models and predictions. On the one hand, large-scale models have gained sufficient maturity over the last decades to provide robust and reliable initial and boundary conditions for regional simulations with an increased resolution (the so-called downscaling approach). On the other hand, oceanographic centers have benefitted from enhanced computing capabilities through the development of high-performance computing technology. Today, short-

Mourre, B., et al., 2018: Assessment of high-resolution regional ocean prediction systems using multi-platform observations: Illustrations in the Western Mediterranean Sea. In "New Frontiers in Operational Oceanography", E. Chassignet, A. Pascual, J. Tintoré, and J. Verron, Eds., GODAE OceanView, 663-694, doi:10.17125/gov2018.ch24.

term (a few days ahead) predictions over extended areas $\mathcal{O}(1000 \text{ km})$ with spatial resolutions of $\mathcal{O}(1 \text{ km})$ and $\mathcal{O}(50)$ vertical levels can be produced sufficiently quickly to be delivered on an operational basis. In parallel, developments in ocean modelling science (e.g., treatment of boundary conditions and sub-grid scale parameterizations) have allowed us to address some of the challenges associated with the increased resolution and its application to coastal areas. These regional implementations are now operated on a routine basis using realistic setups in many regions of the world, often covering open ocean to coastal areas (e.g., Nittis et al., 2001; Wilkin et al., 2005; Siddorn et al., 2007; Chao et al., 2009; Stanev et al., 2011; Kerry et al., 2016; Sakamoto et al., 2016; Kurapov et al. 2017; Kourafalou et al., 2015; and references therein). They aim to reproduce a wide range of spatiotemporal scales, ranging from the variability of the main currents to mesoscale eddies and small-scale features of the coastal circulation such as filaments, coastal eddies or river plumes.

Models provide approximations of reality that are inevitably affected by different types of errors related to inaccuracies in initial and boundary conditions and in the sub-grid scale parameterizations. However, and in spite of this, there is a high demand for products generated from these high-resolution regional models due to their capacity to 1) provide four-dimensional estimates of multiple oceanic variables which are not accessible through observations, and 2) reach coastal zones, raising interest for a diversity of applications. The scientific community uses models to study processes, analyze ocean variability, evaluate energy budgets, or investigate relationships between ocean circulation and ecosystems, for instance. The desire to make informed decisions also motivates the use of models for practical applications. This is the case for search-and-rescue operations, analysis of pollutant drift, science-based management of coastal areas and fisheries, support to ship routing, and forensic science as examples.

Model users from the scientific community and the public have diverse requirements. They might, for instance, ultimately be interested in the strength and direction of the currents over a specific area, their associated variability, the water temperature at the surface and along the vertical, the position and strength of density fronts and eddies, the existence and variability of accumulation zones, the time of residence of water particles in specific areas, or the connectivity between oceanic regions. As a consequence, evaluation of operational model outputs is strongly needed, covering a wide range of different properties (see Hernandez et al., 2015, for a recent review).

Several challenges are associated with the model assessment exercise. First, it is important to keep in mind that evaluation is fundamentally partial since observations are limited in space, time, and variables with respect to the full four-dimensional and multi-parametric extension of the model (Oreskes et al., 1996). This means that only specific properties of the model can be properly evaluated. In particular, high-resolution models produce energetic small-scale oceanic features, such as small eddies and filaments, which are of critical importance for the circulation and energy transfers in the ocean. These structures affect users, in particular through their significant impact on surface currents, but by and large they are not accurately monitored by present observations. Another difficulty is that the model performance generally depends on the region, variable, depth, and spatial and temporal scales under consideration, so that the model assessment presents multiple facets. Moreover, the traditional point-to-point evaluation might become problematic with high-

resolution models where oceanic structures like eddies are present, driven by non-deterministic generation mechanisms, and therefore generally out of sync with the reality. For the structures that can be observed, a small misplacement in time or space in the model generally leads to a large error when using traditional point-to-point evaluation metrics (Ziegeler et al., 2012; Sandvik et al., 2016). Alternative model-data comparison approaches could potentially provide complementary information leading to a fairer evaluation of the simulations. This aspect is illustrated in the second section of this chapter.

From the observational point of view, the developments of operational oceanography and marine technologies has allowed a transition from ship-based observations to multi-platform, integrated observing systems based on moorings, tide gauges, gliders, high frequency radars, drifters, Argo floats, and satellites among other platforms, all providing openly-accessible measurements available in real time. Ocean observatories combine a variety of sampling technologies, which provide access to a diversity of measurements, all with a specific spatial coverage, spatiotemporal resolution, and accuracy. This multi-platform observation paradigm (Tintoré et al., 2013) provides new opportunities for the assessment of numerical simulations based on multiple insights into the skill of the models at different scales. This chapter illustrates such multi-platform model assessment opportunities in the Western Mediterranean Sea, taking as an example the Balearic Islands Coastal Observing and Forecasting System (SOCIB).

The chapter is organized as follows: it first addresses the problem of model performance quantification, highlighting the importance of the choice of the metrics. Then, it introduces SOCIB observatory and model simulations in the Western Mediterranean Sea, before presenting multiple facets of the multi-platform assessment of the model from a qualitative perspective. This chapter is complementary to Chapter 29 by Hernandez et al. in this book, presenting a higher level view of coordinated GODAE and CMEMS (Copernicus Marine Service) model validation activities.

Quantifying Model Performance

In this section, before getting into the details of the Western Mediterranean study case, we first introduce the standard statistical metrics used in model error quantification as well as the potential of alternative approaches.

Standard statistical metrics

Estimating the performance of a model to represent the real state of the ocean commonly goes through the construction of a model equivalent to the available observations. This model equivalent might be a simple interpolation in space and time onto the position of the observations. It may also involve some filtering or grid-cell averaging to mimic the observation process as much as possible. The differences between observations and model equivalents can be quantified using different statistical measures. While the term “error” is used in the following, it is worth mentioning that this

“error” represents model-observation differences, which have contributions from both model and observation errors.

Given vectors of N observation and model values o_i and m_i , with respective standard deviations σ_o and σ_m , we briefly summarize here the most usual statistical quantities computed to assess model performance:

- The Mean Error (ME)

$$ME = \frac{1}{N} \sum_{i=1}^N (m_i - o_i)$$

- The Mean Absolute Error (MAE)

$$MAE = \frac{1}{N} \sum_{i=1}^N |m_i - o_i|$$

- The Root-Mean-Square-Error (RMSE)

$$RMSE = \sqrt{\frac{1}{N} \sum_{i=1}^N (m_i - o_i)^2}$$

- The standard deviation error (SDE)

$$SDE = \sigma_m - \sigma_o$$

- The cross-correlation coefficient (CC)

$$CC = \frac{\frac{1}{N} \sum_{i=1}^N (m_i - \bar{m}_i)(o_i - \bar{o}_i)}{\sigma_m \sigma_o}$$

- From which the cross-correlation error (CCE) can be computed:

$$CCE = \sqrt{2\sigma_m \sigma_o (1 - CC)}$$

There is an important relationship between these quantities allowing to decompose the overall RMSE into different contributions (e.g. Murphy, 1995; Oke et al., 2002):

$$RMSE^2 = ME^2 + SDE^2 + CCE^2$$

The unbiased or centered Root-Mean-Square Error (CRMSE), defined as follows, quantifies the agreement between the fluctuating parts of observations and model values:

$$CRMSE = \sqrt{\frac{1}{N} \sum_{i=1}^N ((m_i - \bar{m}_i) - (o_i - \bar{o}_i))^2}$$

It is linked to other quantities through the following expressions:

$$CRMSE^2 = SDE^2 + CCE^2$$

$$RMSE^2 = ME^2 + CRMSE^2$$

While ME accounts for the mean difference between model and observations, SDE compares the standard deviations of the two fields and CCE, through the cross-correlation coefficient, provides a measure of their general correspondence in phase. Each one of these terms affects the total error provided by the RMSE. A low RMSE is obtained when 1) the mean error is low, 2)

models and observations have similar standard deviations, and 3) the cross-correlation coefficient is close to unity.

The geometric relationships between these quantities allow to represent these multiple statistical measurements of model performance in single summary diagrams such as Taylor (Taylor, 2001) or Target (Jolliff et al., 2009) diagrams. Moreover, skill scores (Murphy, 1995; Willmott, 1981) can also be defined to determine the improvement with respect to specific references such as a climatology, the persistence field, or any other reference simulation. An example of skill score is:

$$SS = 1 - \frac{RMSE^2}{RMSE_{ref}^2}$$

A positive skill score indicates a better performance with respect to the reference (the closer to unity, the better the match with the observations).

Alternative approaches: neighborhood methods

Given a set of observations, these statistical measures of model accuracy using point-wise comparisons are very practical in that they allow provision of single numbers for the model performance. However, the use of point-wise statistics might become problematic when oceanic features (typically an ocean eddy) are represented in the model but with a mismatch in space and/or time with respect to the observations. In this case, the RMSE will be affected by the so-called “double penalty” error, the first penalty being the non-representation of the observed feature and the second the representation of a non-existing pattern. Alternative evaluation methods that have been developed in meteorology (e.g., Casati et al., 2008; Mittermaier and Csimas, 2017) are destined to be more widely used in oceanography in the future to better address these issues. As an illustration of these possibilities, we propose here an alternative evaluation of the performance of different simulations in representing a mesoscale eddy. Fig. 24.1 illustrates a situation where an eddy was observed by altimetry south of Mallorca Island in the Western Mediterranean Sea. Five simulations generated at SOCIB varying model parameters and boundary conditions provide five different representations of sea level anomalies for this date, some of them with an eddy in the neighborhood of the observed structure.

The simulations representing an eddy with similar characteristics to that observed in altimetry, but in a slightly different position, are penalized in terms of RMSE with respect to simulations without any marked eddy. Therefore, an evaluation based on this RMSE might not be a completely fair assessment of the performance of the model.

An alternative framework to evaluate these simulations is provided by neighborhood methods (Ebert, 2009), consisting of characterizing model-data correspondences within space-time neighborhoods not limited to the observation point. In the example shown in Fig. 24.1, the Okubo-Weiss parameter (a particular metric allowing the identification of two-dimensional vortices based on the separation of strain-dominated and vorticity-dominated regions (Okubo, 1970; Weiss, 1991)) has been calculated from the sea level anomalies altimeter map and from the different simulations to focus on the characterization of the eddy. Values of the Okubo-Weiss parameter lower than the

specific threshold of minus two standard deviations (Isern et al., 2003) determines the presence of the eddy in the data and in the simulations. Given a neighborhood distance and a particular grid point where an eddy is detected in the observations, the skill of a simulation for this grid point is here set to one if an eddy is found (from the value of the Okubo-Weiss parameter) in that neighborhood, zero otherwise. The overall skill of a simulation for this specific neighborhood distance is then computed as the spatial average of all local skills computed at every grid point where an eddy is detected in the observations. The overall skill of the different simulations for different neighborhood scales are presented in Fig. 24.2.

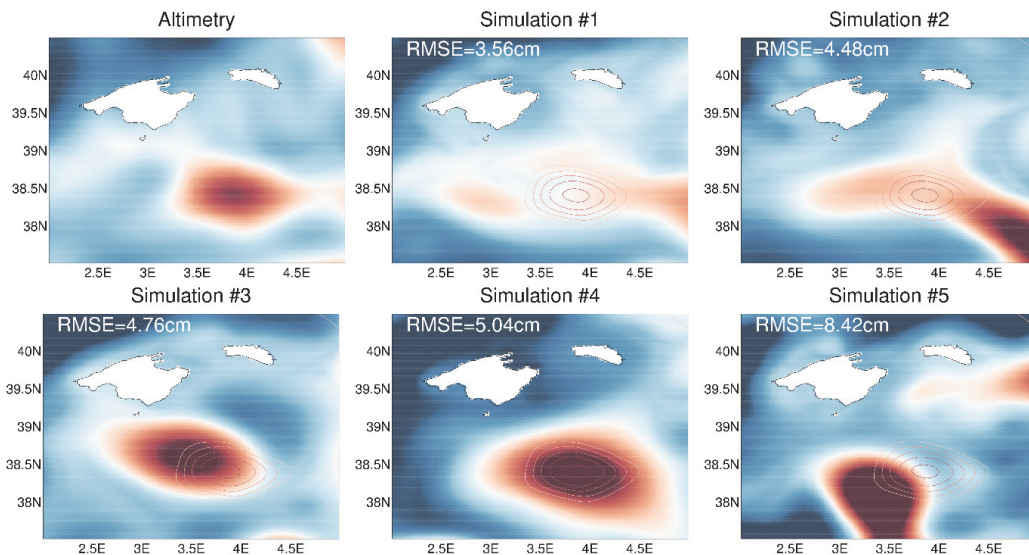


Figure 24.1. Sea level anomalies (cm) from altimetry and five different simulations for 26 September 2014. The point-wise RMSE is specified in the upper-left corner of the simulation panels. The contours of the observed eddy are also plotted in these panels.

Fig. 24.2 shows how simulations 1 and 2, which were the best ranked according to the RMSE, have the lowest skill when using this metric focusing on the representation of the eddy. Simulations 3 and 5 have a maximum skill from 24 km and 44 km distances, respectively. Simulation 4, which represents an eddy centered at the right place but with an overestimation of the radius, exhibits the best skill of all the simulations.

This example illustrates how two different metrics (the standard RMSE and a more sophisticated distance-dependent skill measure focusing on a parameter identifying a specific ocean structure) lead to very different results in terms of model performance. The particular purpose of the use of the model might require the definition of very specific metrics to quantify the model performance.

Other alternatives to point-wise comparisons in deterministic simulations include probabilistic verification approaches, which also aim at dealing with the uncertainty in the location and timing of ocean features. In that framework, an ensemble of model simulations is generated, which allows us to quantify the probability of occurrence of specific oceanic events (e.g., Candille and Talagrand, 2005). Lagrangian methods identifying Lagrangian coherent structures associated with currents, eddies and filaments also provide interesting alternative approaches for the evaluation of high-

resolution models. Lagrangian coherent structure diagnostics allow to detect material surfaces hidden in the ocean circulation (Peacock and Haller, 2013), but with a crucial role on the transport, dispersion and mixing properties of the flow.

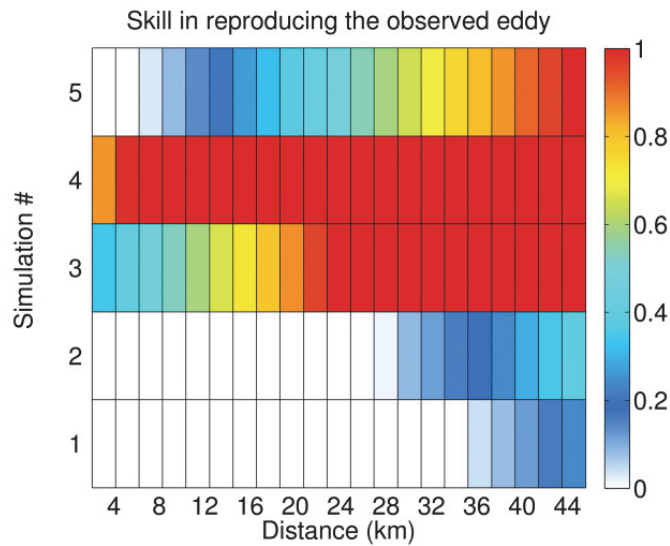


Figure 24.2: Overall skill of the different simulations in reproducing the observed eddy, based on Okubo-Weiss parameter computations and application of a neighborhood approach.

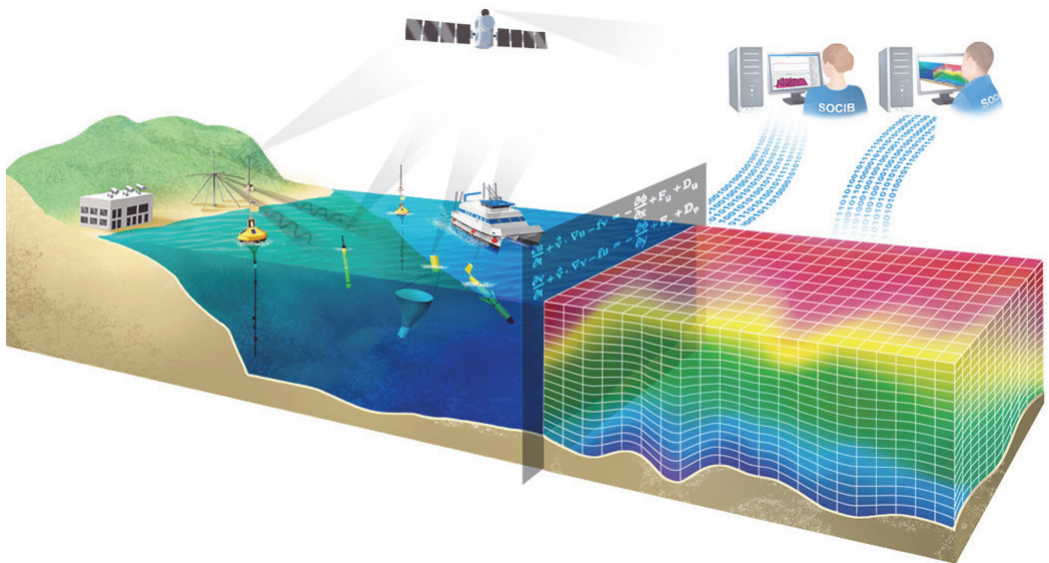


Figure 24.3. Illustration of SOCIB components, with observing facilities (ARGO floats, gliders, research vessel, surface drifters, moorings, beach monitoring, satellites, radars), a modelling and forecasting facility and a data centre for the management and distribution of observations and simulations.

SOCIB Observatory, Study Area, and Modelling System

SOCIB coastal observatory

SOCIB, the Balearic Islands Coastal Observing and Forecasting System (Tintoré et al., 2013), is a coastal observatory located in Mallorca, Spain, with the objectives to collect, quality-control, and distribute multi-platform ocean observations from both fixed and Lagrangian platforms. SOCIB capacities extend from the coastal to the open ocean. In close collaboration with researchers at the Mediterranean Institute for Advanced Studies (IMEDEA, UIB-CSIC), SOCIB aims at supporting research and technology and has a strong orientation towards applications for society. To complement the observations and to provide added-value products, it also produces forecast and hindcast simulations of the ocean circulation, waves, and meteotsunamis affecting the harbour of Ciutadella in Menorca Island. SOCIB multi-platform and modelling components are illustrated in Fig. 24.3.

Circulation and water masses in the Western Mediterranean Sea

SOCIB activities are mainly centred in the Western Mediterranean Sea, which we briefly describe here in terms of its main oceanographic characteristics (see Fig. 24.4 for a scheme of the surface circulation).

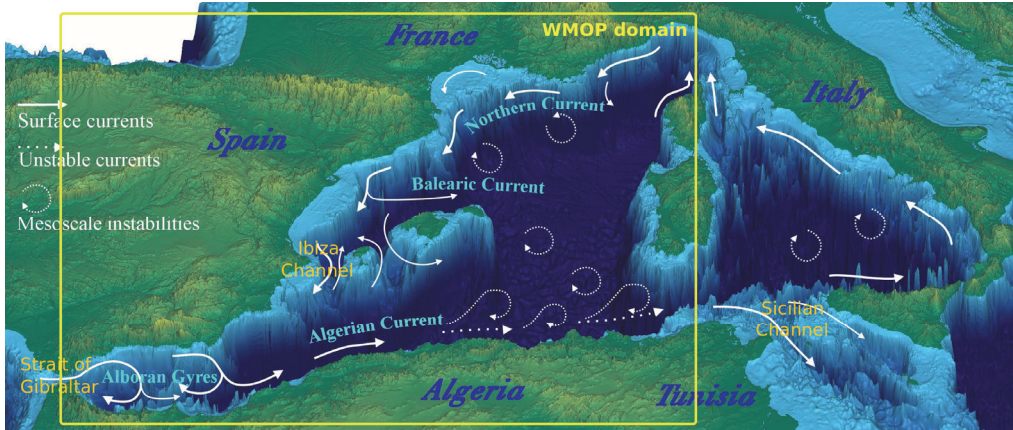


Figure 24.4. Schematic representation of the surface circulation in the Western Mediterranean Sea. The Western Mediterranean Operational Model (WMOP) model domain is indicated in yellow. Adapted from Escudier et al. (2016a) and Millot (1999).

The Western Mediterranean Sea sub-basin is connected to the Atlantic Ocean through the Strait of Gibraltar, where relatively fresh Atlantic Water (AW) is injected with a $\sim 1\text{Sv}$ transport, giving rise to the so-called Atlantic Jet. The Atlantic Jet is an intense meandering and unstable current that interacts with two large anticyclonic gyres in the Alboran Sea until reaching the Almería-Oran front, which separates AW from saltier waters having already recirculated in the Mediterranean Sea. The surface AW then flows along the northern coast of Africa forming the Algerian Current. This current is highly unstable and associated with an intense mesoscale activity. In particular, baroclinic

instabilities generate meanders and eddies that detach from the main flow and propagate along two preferred paths in the southern part of the Western Mediterranean basin (Escudier et al., 2016b). The surface water splits into two branches when reaching Sicily. The first branch crosses the Sicilian Channel and flows cyclonically towards the Eastern Mediterranean Basin where it becomes more saline due to intense evaporation. The second branch flows to the north along the western coast of Italy through the Tyrrhenian Sea. This northward current converges north of Corsica with the Western Corsica Current to give rise to the Northern Current, which flows westwards along the shelf break until reaching the Balearic Sea. It then splits into two branches: the Balearic Current flows north-eastwards along the northern shelf of the Mallorca and Menorca islands, also fed by AW inflows through the Ibiza and Mallorca channels, and the remaining part flows southwards through the Ibiza Channel into the Algerian Basin. Further details can be found in Millot (1999), Millot and Taupier-Letage (2005), or Robinson et al. (2001).

Different water masses are found in the Western Mediterranean Sea. At the surface, the relatively fresh AW becomes progressively more saline along its path in the Mediterranean basin under the effects of evaporation. In particular, two types of AW can be distinguished in the Balearic sub-basin according to their salinity: 1) AW of recent Atlantic origin that flows from the south (AW_r, salinity < 37.5), and 2) more saline AW having circulated in the Western Mediterranean Sea and flowing from the north (AW_o, salinity > 37.5). At the intermediate levels, a warm and salty Levantine Intermediate Water, which originates from convection processes in the Levantine sub-basin of the Eastern Mediterranean Sea, enters the Western basin through the Sicilian Channel at depths between 200 and 500 m. A second intermediate water mass, relatively cold and fresh and known as the Western Intermediate Water, is formed during winter cooling events in the Gulf of Lion, Ligurian Sea, or Ebro river area. This regional winter water mass flows southwards between AW and Levantine Intermediate Water, intermittently reaching the Ibiza Channel. The Western Mediterranean Deep Water is found at deeper levels (>1000 m), formed during extreme winter weather events leading to deep convection in the Gulf of Lion.

The Mediterranean Sea is often considered as a reduced ocean laboratory for ocean studies, due to the presence of ocean processes of global relevance such as mesoscale and submesoscale activity, eddy propagation, water mass formation and spreading, and the smaller Rossby radius (~10-15 km) compared to the large oceans. In particular, the narrow Ibiza Channel (850 m deep and 90 km wide), and to a lesser extent the Mallorca Channel (650 m deep and 80 km wide), represent key “choke points” for the north/south exchanges of the different water masses, and concentrate signals from different processes including surface circulation, mesoscale activity, and intermediate water mass formation and propagation. This is the reason why they have been the focus of specific regional sampling programs, including a glider endurance line operated by SOCIB since 2011.

Modelling system

The Balearic Sea is a particularly challenging region for ocean modelling due to the complexity of the topography and the interaction of multiple ocean processes, in which salinity gradients in

particular play a key role. To simulate the ocean circulation and mesoscale variability in the Balearic Sea and adjacent sub-basins, SOCIB runs the Western Mediterranean Operational Model (WMOP, Juza et al., 2016). WMOP provides both daily predictions and hindcast simulations over the recent years. The model has a spatial resolution of 2 km, and is nested in the larger-scale 1/16° Mediterranean model from the Copernicus Marine Service (CMEMS-MED, Clementi et al., 2017; Simoncelli et al., 2014) through a dynamical downscaling approach. WMOP uses a regional configuration of the ROMS (Shchepetkin and McWilliams, 2005) model covering an area from the Strait of Gibraltar to the Sardinia/Corsica Islands. The vertical grid is made up of 32 stretched sigma levels. The high resolution HIRLAM atmospheric fields (Undén et al., 2002) from the Spanish Meteorological Agency are used to compute surface fluxes through bulk formulae. They have a resolution of 5 km in space and 1 hour in time. Runoffs from the six major rivers of the domain are also specified as point sources of low saline water with their corresponding volume transports. The vertical mixing is determined in the model using the generic length-scale method described in Umlauf and Burchard (2003). At the boundaries, mixed active-passive conditions (Marchesiello et al., 2001) are imposed using daily forcing data from the CMEMS-MED simulations. A particular treatment, including the alignment of bathymetries between the external model and WMOP and a correction of interpolated velocities, is applied at the Strait of Gibraltar to ensure that the boundary forcing field properly represents the original inflow and outflow transports of the large-scale model.

Near real-time & Delayed mode

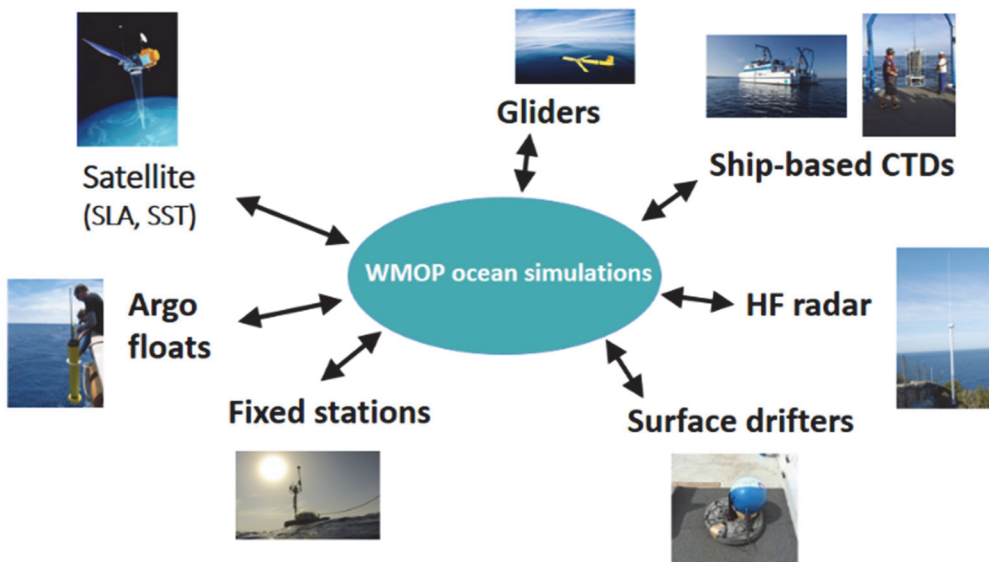


Figure 24.5. Multi-platform observations used for WMOP model evaluation in near real-time and delayed modes.

The model is run in both hindcast and forecast modes. None of them include data assimilation at the moment. On the one hand, free run hindcast simulations (hereafter the *WMOP_hindcast*) are performed over the period 2009-2015 using initial and boundary fields from the CMEMS

Mediterranean Sea physical reanalysis (CMEMS-MED-REAN, Simoncelli et al., 2014), with an initialization on 15 September 2008. Observed daily river discharge values are prescribed in the *WMOP_hindcast*. These free-running simulations are mainly used for detailed studies of dynamical ocean processes.

On the other hand, WMOP forecasts use the CMEMS Mediterranean Sea Analysis and Forecast products (CMEMS-MED-AN-FC, Clementi et al., 2017) and climatological values of river discharges to provide daily operational 72-hour predictions (hereafter the *WMOP_forecast*). *WMOP_forecast* is reinitialized every week from the output of a three-week spin-up simulation initialized from the CMEMS-MED-AN-FC model fields. This regular restart aims to avoid significant drifts of the model in the absence of data assimilation. The *WMOP_forecast* uses climatological values of river discharges. Both the *WMOP_hindcast* and *WMOP_forecast* use HIRLAM outputs as atmospheric forcing.

Multi-platform Model Assessment in the Western Mediterranean Sea

WMOP ocean simulations are systematically compared to multi-platform observations from satellite, SOCIB platforms, and other national and international ocean monitoring systems, both in real-time and delayed modes (Fig. 24.5). In particular, the *WMOP_forecast* model-data comparisons are updated daily on SOCIB website (www.socib.es). In the following section, we illustrate the multiple possibilities of model assessment provided by these different platforms, remaining intentionally qualitative in the evaluation. Yet, all types of model-data comparisons illustrated in this section can be quantified through the standard statistical measures introduced in Section 2 or through any other specific metrics.

Satellite altimetry and Mean Dynamic Topography

Satellite altimeters are unambiguously essential ocean observing platforms that enable repetitive and global measurements of sea level anomalies with respect to a long-term mean. These sea level anomalies provide estimates of the variability of surface geostrophic currents. Furthermore, advanced methods combining altimeter time series, hydrographic profiles, and long-term model averages allow to estimate the Mean Dynamic Topography (MDT), i.e. the long-term mean sea level elevation with respect to the marine geoid. This, in turn, allows for provision of accurate estimates of the mean surface geostrophic circulation over the period of a model simulation. Note that the MDT is not directly measured by the altimeter, but instead estimated from a combination of observation and model data sources. The scarcity of measurements in specific areas might still lead to uncertainties in this estimate of the mean circulation. The comparison of the mean model sea surface with the MDT allows us to evaluate the large-scale mean circulation in the model, which is an essential aspect to be verified before considering further details. Also note that the MDT provides mean sea level elevations over a reference period. When the period of the model simulation

differs from this reference period, this mean state needs to be corrected by the mean altimeter anomalies over the simulation period to represent the mean dynamic topography over the same period as the numerical simulation.

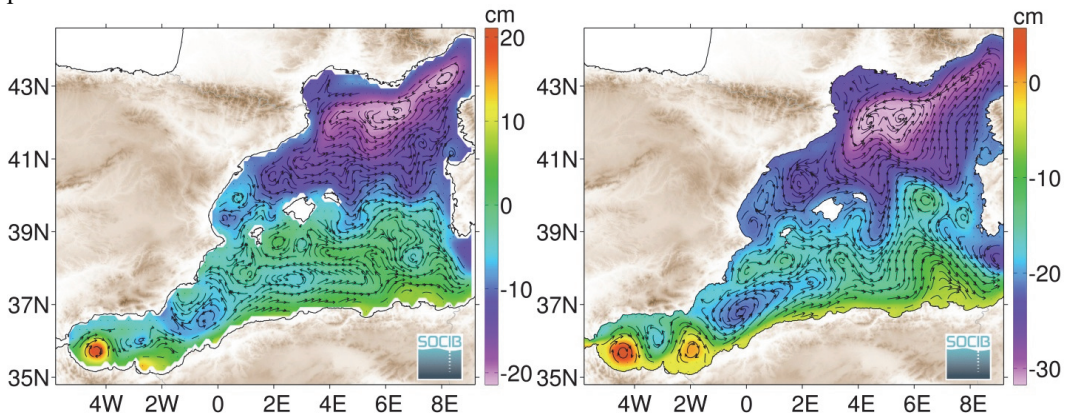


Figure 24.6. Mean absolute dynamic topography and associated surface geostrophic currents over the period 2009–2015. Left: from the MDT (Rio et al., 2014) corrected by mean altimeter anomalies over the period 2009–2015; Right: from the *WMOP_hindcast* simulation.

The comparison displayed in Fig. 24.6 shows that the regional WMOP model is able to properly represent the mean surface circulation, including the Atlantic Jet, the western and eastern Alboran gyres (with a stronger signal of the eastern Alboran gyre with respect to the MDT), the Algerian Current, the cyclonic circulation in the Ligurian Basin and Gulf of Lion, and the Northern and Balearic currents. Details of eddies and meanders differ between the two estimates, especially in the Algerian Basin. Similar analyses with other Western Mediterranean Sea models can be found in Pascual et al. (2014) and Escudier et al. (2016a). Note that the color bars in both panels have the same range but are not centered on the same values. Indeed, here the model mean sea level is mainly determined by initial and boundary conditions coming from the larger scale CMEMS-MED-REAN model and does not necessarily match the mean sea level provided by the MDT. The relevant aspects of the comparison concern the spatial variability and the associated gradients of the mean sea surface height, which determine the mean ocean circulation. The mismatch between the spatial mean model sea surface and the MDT will, however, require special care when assimilating data in the model.

The fundamental strength of altimetry is its ability to measure the variability of the sea level around this mean state. In particular, sea surface height variance or eddy kinetic energy (EKE) computed from the altimeter-derived geostrophic currents allows us to quantify the energy associated with the mesoscale activity. Fig. 24.7 shows several estimates of the EKE from a) altimeter-derived geostrophic velocities (calculated from the daily $1/8^\circ$ -resolution, delayed-time, all-sat-merged Mediterranean Sea gridded product distributed by CMEMS); b) total model velocities; c) model surface geostrophic velocities; and d) spatially- and temporally-filtered model surface geostrophic velocities to remove the effects of the small scales unresolved by altimetry.

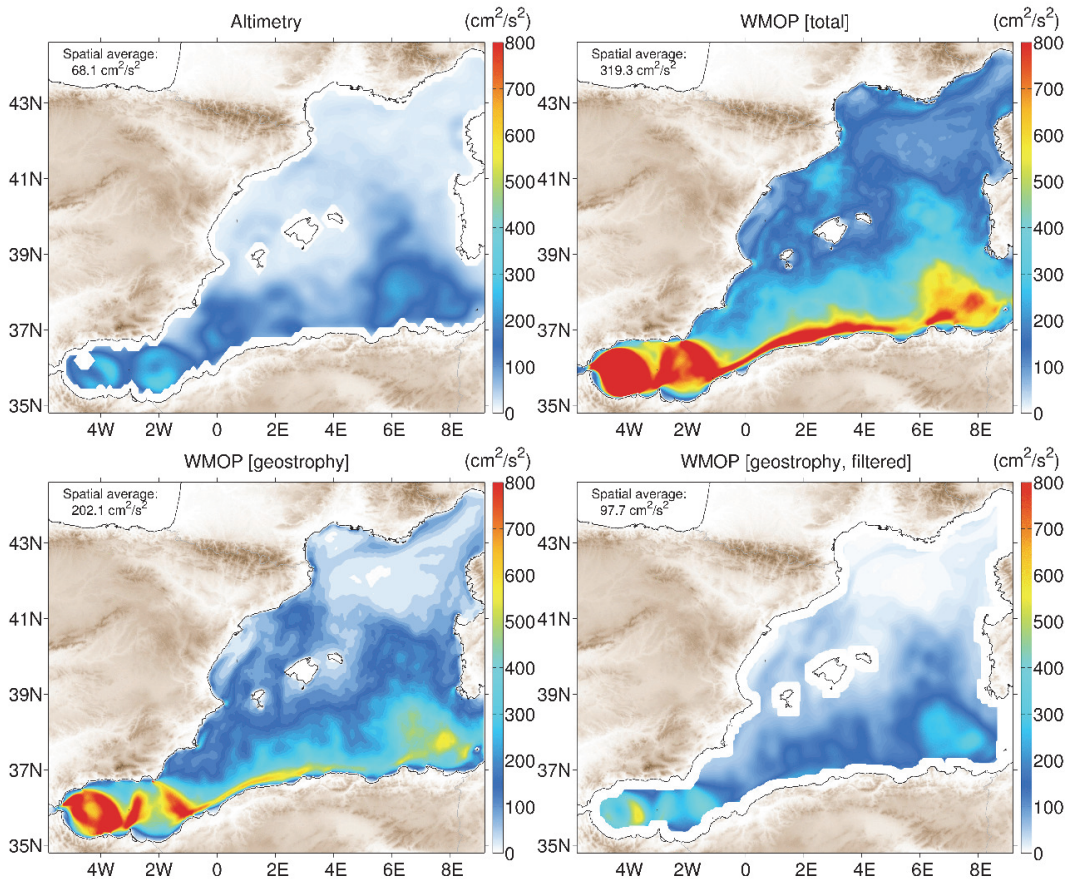


Figure 24.7. Mean eddy kinetic energy (EKE) over the period 2009–2015, from: a) gridded altimetry; b) *WMOP_hindcast* total surface currents; c) *WMOP_hindcast* geostrophic surface currents; d) *WMOP_hindcast* filtered (44 km and 10-day moving average) geostrophic surface currents.

Comparisons of the different panels reveal that the eddy activity is larger in the southern part of the model (Alboran Sea and Algerian Basin), both in the model and altimeter estimates. However, the mean EKE is found to be more than two times larger in the total model velocities than in the altimeter-derived geostrophic currents. Indeed, the high-resolution model represents 1) ageostrophic processes and 2) energetic small eddies and filaments associated with the mesoscale structures, which are not present in the altimeter estimates. Gridded altimetry is only able to represent the geostrophic mesoscale activity associated with oceanic structures with a minimum radius around 40–50 km (Chelton et al., 2011), only allowing us to evaluate the realism of the model at those scales. Comparisons of panels b) and c) illustrate the importance of the ageostrophic component in the total model surface currents. The EKE is reduced by up to 40% in the energetic areas of the Alboran Sea and Algerian Basin. When the model surface geostrophic velocities are filtered to remove the impact of small spatiotemporal scales that are not resolved by altimetry (panel d), the EKE gets much closer to that provided by altimeter estimates, indicating a realistic amount of mesoscale variability of the model at these scales. In the model assessment exercise, the representativity of model estimates with respect to specific observations needs to be properly taken

into account to interpret model-data differences. Here, only complementary data from surface drifters and high frequency (HF) radar would allow us to assess the realism of the model EKE at the smaller scales.

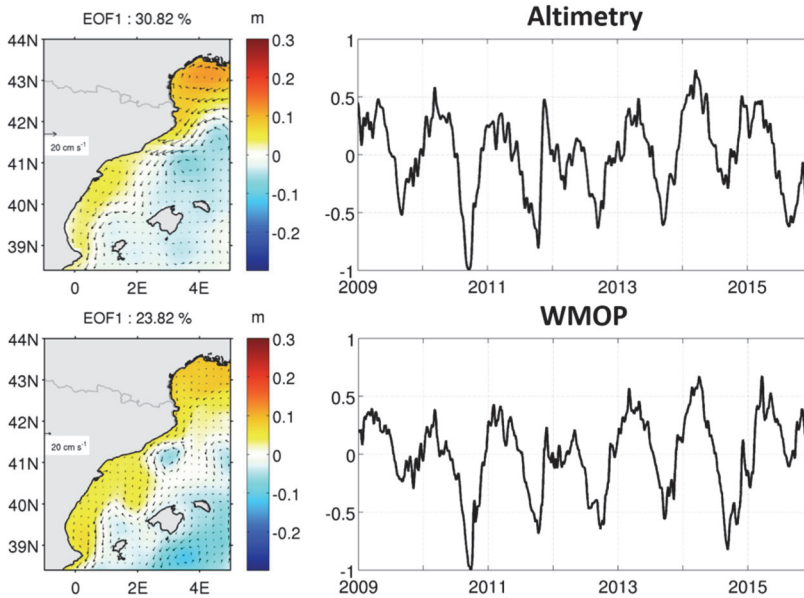


Figure 24.8. First empirical orthogonal function (EOF) mode of sea level anomaly variability from altimetry (upper panels) and *WMOP_hindcasts* (lower panels). Left: spatial pattern and explained variance; Right: associated time series.

Sea level map time series available through altimetry are also frequently analyzed in terms of empirical orthogonal functions (EOFs), which consist of decomposing the signal in terms of orthogonal basis functions (e.g., Emery and Thompson, 2001). As a result of this analysis, a set of dominant spatial patterns of variability can be identified together with their corresponding time series. Fig. 24.8 illustrates one such analysis, comparing the first EOF mode of sea level anomalies variability from altimetry and from the model, in terms of spatial pattern and corresponding temporal coefficients. In both cases, this mode is associated with an acceleration (when the associated coefficient is positive) or deceleration (when the coefficient is negative) of the slope current.

This comparison shows that the main mode is associated with the velocity of the slope current in both cases, but with some differences such as a larger variability in the Gulf of Lion in the observations and the significant signature of an eddy north of Mallorca in the model. Both time series have a strong seasonal component with a good correspondence in phase, modulated by a significant interannual variability. The deceleration of the Northern Current in 2010, characterized by a significant negative value of the EOF coefficient is well represented in the model. EOF patterns and associated time series are useful diagnostics to detect whether the model properly captures the main dynamical properties in the area of study.

Other sophisticated analyses of sea level signals can be carried out to evaluate the model performance. For instance, along-track altimeter and model data can be analyzed in terms of sea

level wavenumber power spectra to examine the energy distribution across different scales (e.g. Le Traon et al., 2008). Finite size Lyapunov exponents computations in the model and the data can also be applied to evaluate the representation of Lagrangian coherent structures associated with eddies and fronts in the model. Here, we illustrate another advanced analysis consisting of characterizing eddies using an automatic detection method.

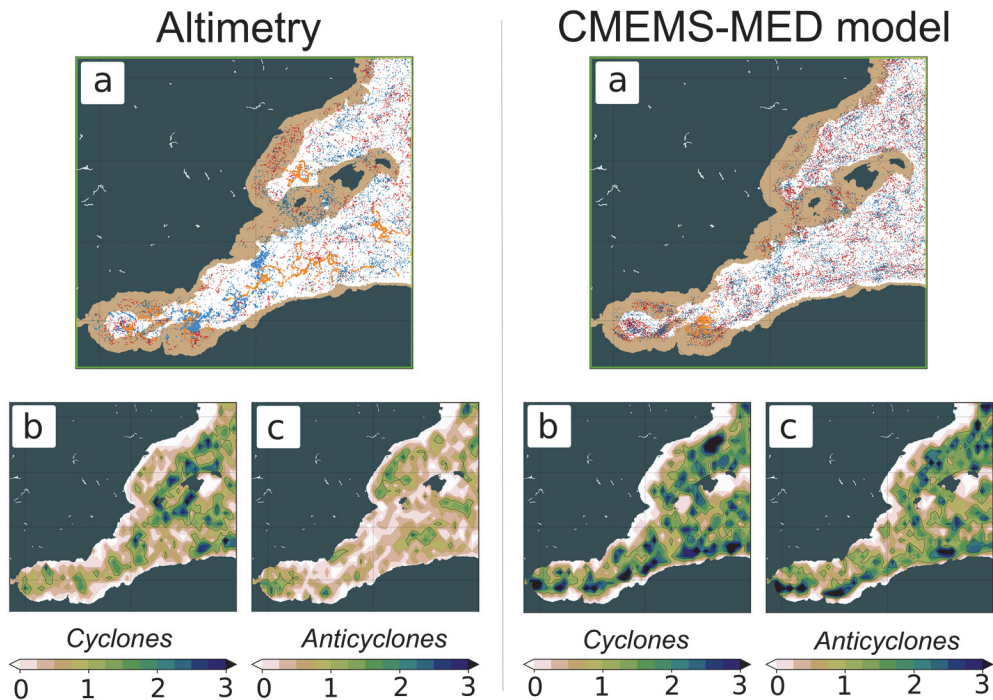


Figure 24.9. Selection of eddy properties in the western Mediterranean from altimetry and the CMEMS-MED-AN-FC model between 2013 and 2016. (a) Cyclone (blue) and anticyclone (red) eddy tracks detected in the altimetry and the model. Light blue and orange markers indicate eddies with lifetimes greater than six months (cyclones and anticyclones, respectively). Bottom: eddy counts per $0.2^\circ \times 0.2^\circ$ bins per year for altimetry and CMEMS-MED-AN-FC model for (b) cyclones and (c) anticyclones.

Indeed, the availability of sea level altimetry maps has motivated the development of these automatic eddy detection methods based on either closed contours of sea level anomalies, geometry of surface velocities, or local deformation properties of the flow (Chelton et al., 2011; Nencioli et al., 2010). They allow quantification of the number, position, polarity, amplitude, size, and lifetime of eddies, which provides an alternative and novel view of the mesoscale variability that can also be evaluated in model outputs (Halo et al., 2014; Escudier et al., 2016a).

The examples given here use the automated eddy tracker *py-eddy-tracker* (v3; Mason et al., 2014), which analyzes sea surface height fields, searching for closed contours that are associated with the surface signature of eddies. The method is applied here to altimetry and to the CMEMS-MED-AN-FC model, which is used as the “parent” model of the *WMOP_forecast* simulations. Fig. 24.9 shows eddy locations for cyclones (blue) and anticyclones (red) from altimetry and for the CMEMS-MED-AN-FC model over the period 2013–2016. Eddies are present over the whole

domain, with higher densities in the Algerian basin, especially around longitude 0°, where instabilities of the Algerian current occur (Millot, 1985, Escudier et al., 2016b).

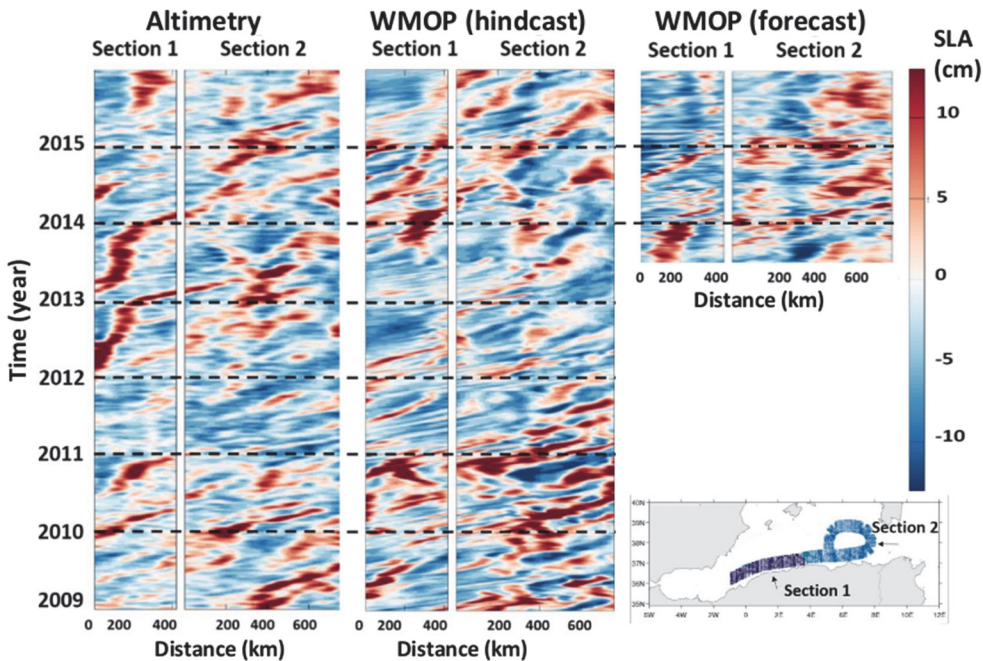


Figure 24.10. Hovmöller diagrams of sea level anomalies along sections 1 and 2 of Algerian eddy propagation paths for altimetry, *WMOP_hindcast* and *WMOP_forecast* simulations.

Eddy counts from the eddy tracker are higher from the model than those from altimetry, for both cyclones and anticyclones. This result is to be expected given the higher resolution of the model compared to altimetry. Furthermore, the presence of eddies in gridded altimetry products was shown to be affected by the particular position of satellite tracks (Escudier et al., 2016a), which does not happen in the model. These advanced automatic detection methods have been successfully applied with gridded altimeter data in many regions of the world oceans, while also highlighting different outcomes between distinct detection methods in some cases (Escudier et al., 2016a, 2016b). Their application to high-resolution models representing smaller and highly dynamic eddies is relatively recent and probably still requires a special attention in the interpretation of the results.

Eddy statistics derived from the application of multiple eddy trackers to altimeter map time series have permitted the identification of eddy propagation paths in the Algerian Basin (Escudier et al., 2016b). Algerian eddies preferentially propagate around two gyres with two marked detachment points from the African coast. Once these propagation paths have been identified, Hovmöller diagrams of sea surface anomalies along these paths allow us to analyze the presence and propagation of eddies and evaluate these particular aspects in model simulations. Fig. 24.10 presents such an analysis for altimetry maps, *WMOP_hindcast* and *WMOP_forecast* models. Even if the number of eddies generated in the model along section 1 (see map in lower right corner of the figure) is quite consistent with the observations (one large eddy per year with a significant interannual variability), as well as the propagation speed of these eddies, their timing is not properly

represented in the model. This comparison indicates that instabilities of the Algerian current occur in the model, but the proper representation of particular eddies and meanders needs to be constrained through data assimilation.

Finally, it is worth mentioning that the advent of high-resolution altimetry, including delay-Doppler/SAR (synthetic aperture radar) technology, Ka-band missions, 20Hz high-sampling rate signals, or the forthcoming SWOT wide-swath instrument, all providing an enhanced capacity to approach closer to the coast, also offers new capabilities to evaluate the smaller-scale features represented in high-resolution ocean models.

Satellite sea surface temperature

Sea surface temperature (SST) is a key ocean variable routinely observed by satellites with a global coverage and high resolution. By measuring the radiation emitted by the ocean surface, thermal infrared and passive microwave radiometers provide SST images with different resolution, accuracy and spatiotemporal coverage due to the specific influence of clouds and other atmospheric effects. Advanced optimal interpolation and blending allow to combine the measurements from different satellites and provide improved gap-free SST products (e.g., GODAE High-Resolution SST GHRSSST project) that are useful for model validation. Model-data SST comparisons allow us to evaluate the representation of air-sea interactions and vertical mixing in the model and provide indications on the validity of both model parameterizations and external forcing fields. High-resolution SST is also useful to monitor mesoscale structures like eddies, fronts, or filaments since these structures often have significant signatures in temperature.

The use of combined products provides access to gap-free SST time series allowing us to precisely assess the seasonal cycle in the model, the main modes of variability through EOF analysis, or the regional distribution of model surface temperature errors. In cloud-free areas, the use of images from infrared radiometers might be more adapted when focusing on the evaluation of specific mesoscale and submesoscale features due to their high resolution (~1km) and accuracy, which allows for the precise identification of surface temperature gradients associated with fronts and filaments. Advanced detection algorithms (e.g., Belkin and O'Reilly, 2009) can be applied to both satellite imagery and model outputs to evaluate the representation of oceanic fronts in the model. One aspect to be considered when comparing model and satellite SSTs is that these estimates do not generally represent the temperature at the same effective depth. On the one hand, infrared and microwave radiometers measure the so-called skin and sub-skin SST, which correspond to depths around 10 μm and 1 mm, respectively. The foundation SST, which corresponds to nighttime SST free of any diurnal variability at a depth around 10 m, is often provided in blended products. On the other hand, the effective depth of the model SST depends on the thickness of the uppermost level. Fig. 24.11 illustrates the richness of satellite SST data, showing an example of comparisons of SST with the *WMOP_forecast* and Level-4 optimally interpolated product from CMEMS (Buongiorno-Nardelli et al., 2012) for a specific day on 19 September 2017.

It shows good overall agreement between the two fields, with differences in the small-scale features associated with the frontal areas, in the coastal zones of the Gulf of Lion under the influence of upwellings and the Rhône river discharge, and in the Alboran Sea where the absence of tidal mixing in the model tends to generate an overestimation of the SST. Notice the representation of many details in the observed SST field, such as the long filament of relatively colder water with respect to the surroundings extending south of Ibiza Island towards the African coast around 2°E.

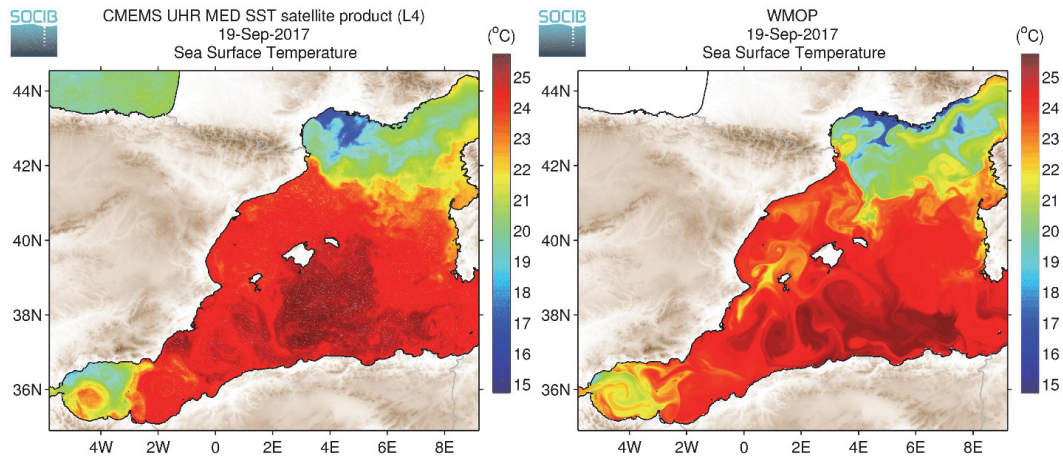


Figure 24.11. Sea surface temperature (SST) on 19 September 2017 from a) a satellite-derived optimally interpolated product distributed through CMEMS, and b) the *WMOP_forecast* model.

Argo floats

Argo floats are Lagrangian platforms that provide regular profiles of the upper thermohaline structure in the ocean, allowing a vertical characterization that is complementary to surface satellite measurements. In the Mediterranean Sea, Argo floats are programmed to execute five-day cycles. SOCIB participates in the Argo program, deploying several floats each year. At the time of the writing of this chapter, there were 63 floats distributed over the whole Mediterranean Sea, 25 of them located in the Western Mediterranean sub-basin. This system provides an average of five profiles per day with a random distribution over the domain. The distance between two profiles is on the order of 200-300 km. While Argo profiles do not allow us to characterize small-scale variability, they are very useful in assessing the seasonal and interannual variations of water mass properties over the basin. They provide estimates of vertical stratification and mixed layer depth and so they can be used to evaluate the vertical mixing properties in the model. They might also be used to test the performance of the model in representing intermediate and deep water masses after convection events that are parameterized in the model. Argo floats provide systematic salinity data, which is an essential variable affecting sea water density and ocean circulation and of particular importance in the Mediterranean Sea. This is highly valuable for the assessment of ocean models, which are generally found to be affected by significant errors in the representation of ocean salinity. Fig. 24.12 illustrates Argo-model comparisons available for a specific day in September 2017, allowing us to evaluate the realism of the model mixed layer and thermocline in particular. In the

recent years, the Argo program has been extended to include biogeochemical observations. More than 100 Biogeochemical-Argo profiling floats were deployed in the world oceans, providing measurements of oxygen, nitrates, chlorophyll fluorescence, or particulate backscattering. The Mediterranean Sea is one of the regions with the densest network of Biogeochemical-Argo floats.

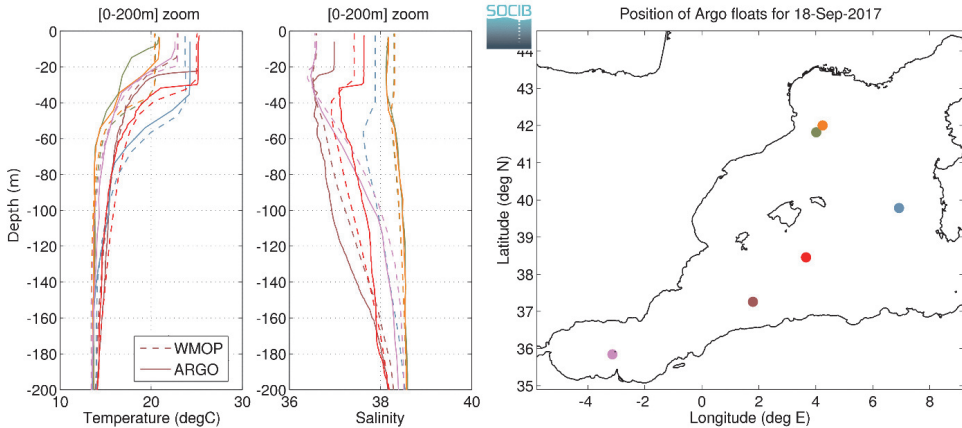


Figure 24.12. Temperature and salinity vertical profiles from Argo and from the *WMOP* forecast on 18 September 2017.

Fixed moorings

Moorings offer the capability to measure multiple ocean variables at a fixed location over long time periods. They allow us to characterize both high-frequency variability, sporadic events, and longer period signals at a wide range of timescales on the shelf and in the coastal area. Fixed moorings can be equipped with CTDs, acoustic Doppler current profilers (ADCPs) or thermistor chains to provide measurements of temperature, salinity, and velocities at different depths. They also frequently host meteorological instruments. SOCIB maintains two fixed moorings, in Ibiza Channel and in the Bay of Palma, that are complementary to other stations operated by Puertos del Estado along the continental slope of the Iberian Peninsula. Measurements from fixed moorings can be used to verify whether the model properly represents the frequency content of the variations of oceanic properties. They can also be used to identify and analyze specific events in the time series. When equipped with meteorological sensors, they might provide insights into the realism of air-sea fluxes in the model. Importantly, moorings are also platforms used to collect biogeochemical measurements.

The left panel in Fig. 24.13 illustrates the evolution of SST over a one-month period. It shows an overall decrease in the SST associated with the seasonal cycle, combined with 1) SST variations over the atmospheric weather scale of a few days and 2) the daily warming cycle due to solar radiation. On the longer timescale (right panel), the seasonal cycle and interannual variations are also precisely measured by the instrument and can be evaluated in the model, illustrating how model-data comparisons can be used to evaluate the model performance at these different scales. Moorings equipped with temperature and salinity sensors along the vertical also allow to monitor the variability of the mixed layer depth and to precisely evaluate vertical mixing properties in the model.

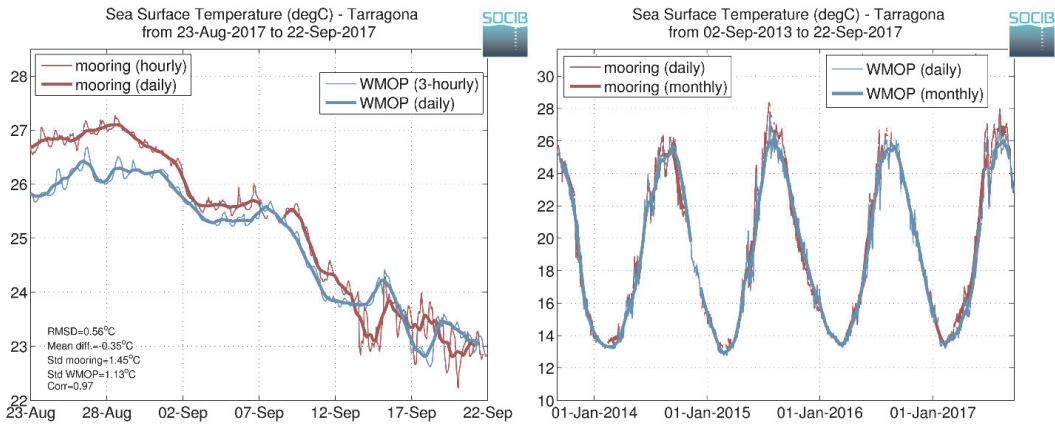


Figure 24.13. Time series of sea surface temperature from the *WMOP* forecast model and mooring data at Tarragona station (northernmost mooring in Fig. 24.15): a) over a one-month period from 23 August to 22 September 2017; b) over a four-year period from 02 September 2013 to 22 September 2017.

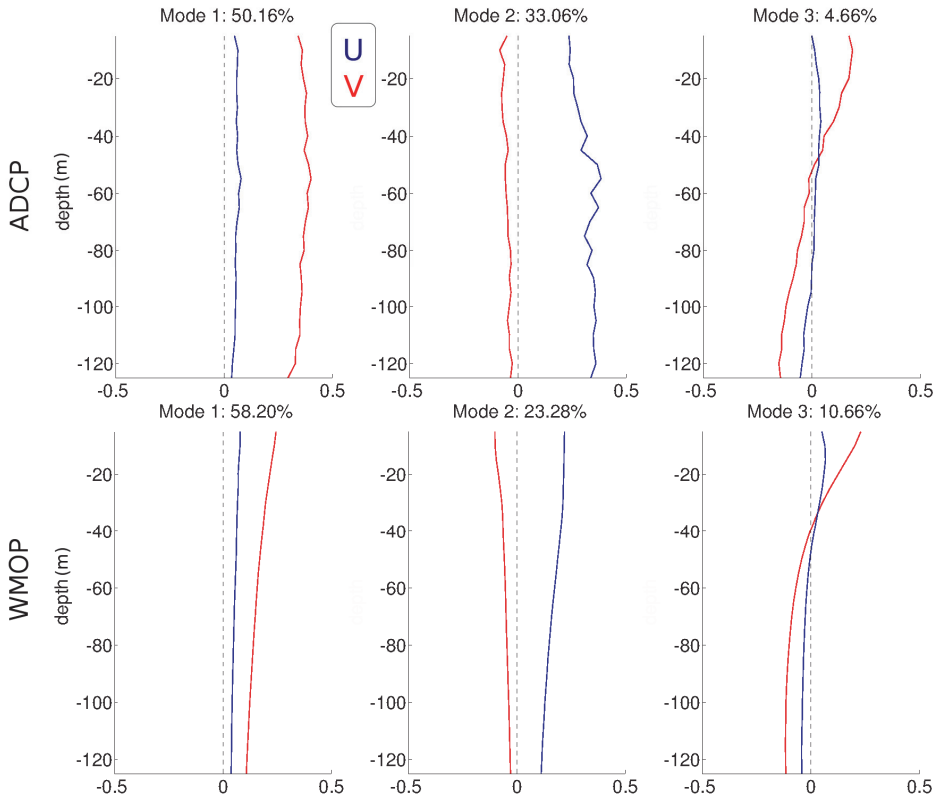


Figure 24.14. Three main modes of vertical EOF patterns for ADCP observations and the *WMOP* hindcast at Ibiza Channel mooring. The meridional component of the velocity is plotted in red, the zonal component in blue.

Moorings often host current meters and ADCPs, providing time series of ocean velocities at different depths. These time series along the vertical can be analyzed in terms of EOFs to determine the vertical modes of variability. The vertical EOFs shown in Fig. 24.14 are qualitatively close to each other between model and observations: a first mode mainly representing the meridional variability with a small zonal component, a second mode representing the zonal variability, and a third mode with a marked baroclinic structure and a zero-crossing around 40 m depth. The modes have the same order of magnitude in the model and observations. A noticeable difference is the decay of the variability of velocities with depth in modes 1 and 2 in the model, which is not depicted in ADCP observations. This comparison provides unique information about the capability of the model to represent the variability patterns along the vertical. Cross-correlations between different depths can also be estimated from the ADCP data, providing an assessment of vertical model correlations used in data assimilation schemes, for instance (Oke et al., 2002).

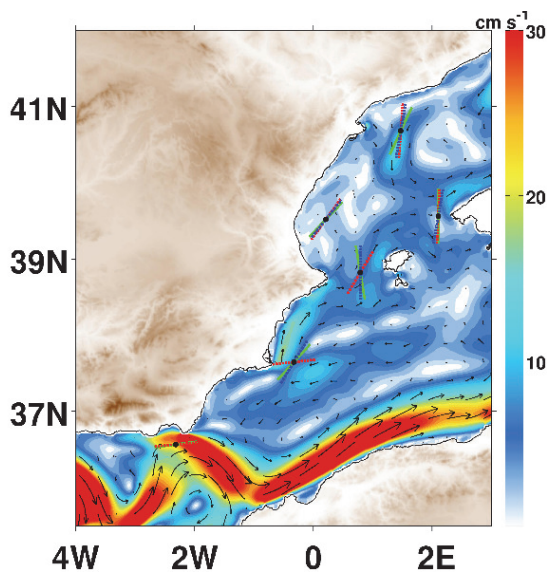


Figure 24.15. Main axes of variability computed at different mooring locations along the Iberian shelf break (moorings operated by Puertos del Estado in Tarragona, Valencia, Dragonera, Cabo de Palos and Cabo de Gata, and SOCIB in the Ibiza Channel), plotted over the mean velocities of the *WMOP_hindcast* simulation. Blue: mooring, Green: altimetry, Red: the *WMOP_hindcast*.

The computation of the main axis of variability is another example of how we can exploit fixed location measurements to evaluate the model currents. The availability of current time series from moorings allows us to determine the axis along which the variance in the observed velocity fluctuations is maximum. The angle of maximum variance can also be computed from the model and compared to the observational estimates. In the comparison presented in Fig. 24.15, model and data are found to be in general good agreement. Discrepancies between model and mooring data of about 20° in terms of mean axis orientation are found in Ibiza Channel and Cabo de Palos moorings, highlighting errors in the variability of the surface circulation in the model. Altimeter estimates coincide with mooring data except at Tarragona station where the model slightly better matches the mooring than altimetry.

Surface drifters

Hourly surface ocean velocities can be obtained from surface drifters, providing essential information for model validation. Surface drifters are driven by the total currents including the contributions of winds, waves, mesoscale and submesoscale structures, tides, or inertial oscillations. They provide a complementary source of information on surface currents with respect to altimetry, which is limited to the geostrophic component and larger scales. When deployed in coastal areas they provide details of the circulation that are generally not accessible from other observations except in areas covered by HF radars. Surface drifters often have a drogue so that they drift according to the currents at a specific depth (a few meters below the surface); this needs to be carefully taken into account before comparing with model currents. Eulerian model-data validation using drifters is possible if a sufficient number of floats is available to map the currents over a specific area. An illustration is provided in Fig. 24.16, computing mean values of the velocities at 15 m depth from a set of 33 drifter trajectories over spatial bins of $0.1^\circ \times 0.1^\circ$.

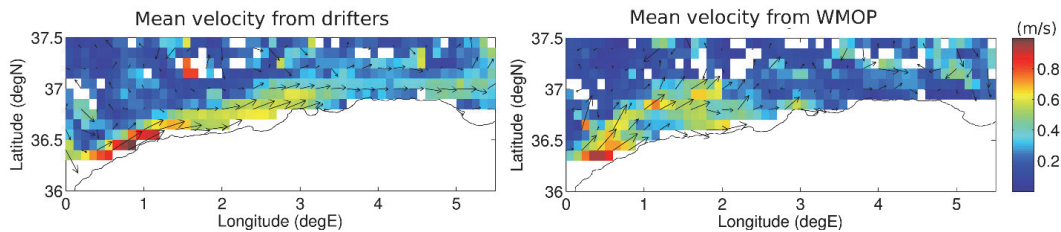


Figure 24.16. Left: mean Eulerian velocity fields computed from 33 drifter trajectories with a drogue at 15 m depth in the Algerian Basin during the period 2011–2015. Right: mean velocity fields at 15 m depth from *WMOP_forecast* simulations sampled at the time and locations of the drifters.

Fig. 24.16 depicts values of drifter velocities larger than 0.6 m/s along the Algerian coast west of 3°E . Such values are also found in the *WMOP_forecast* but the current has a wider extension with respect to the data. Moreover, while the current continues to drive the drifters east of 3°E with a velocity around 0.3–0.4 m/s, it appears to fluctuate more in the model. One important limitation here is that the reliability of Eulerian statistics inferred from surface drifters is limited by the amount of available drifters. Also, the distribution of real drifters might be biased by a convergence effect attracting the drifting floats towards the areas of larger velocities (Davis, 1985).

The most common way to compare drifter data with models is to use Lagrangian diagnostics based on the comparison of observed and modeled trajectories. Virtual drifters can be launched in the model from the real position of the platforms and advected by the model velocities, including a diffusive component to represent the effect of unresolved processes. The evolution of separation distances with time between model and real trajectories then provides an evaluation of the model surface velocity errors (e.g. Liu and Weisberg, 2011).

Fig. 24.17 illustrates how drifters can be used to evaluate two different coastal processes in the model. First, the presence of a coastal gyre close to the northern cape of Mallorca Island is revealed by the trajectory of two drifters, with a good correspondence with model surface velocities. In the second example, the model is found to properly represent the mean current direction and magnitude over a three-day period, in particular also including cross-shore oscillations associated to sea breeze

effects in the Bay of Palma. This evaluation of coastal processes is very valuable for applications based on surface drifts such as search-and-rescue or responses to local emergencies on short timescales. Notice that the SST is also generally recorded along the drifter trajectory and can be used for a complementary model validation.

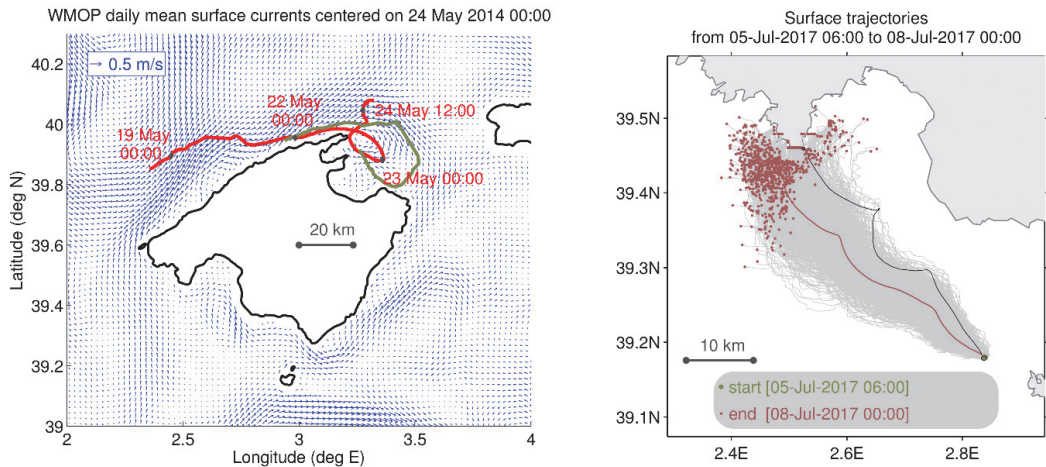


Figure 24.17. Left: An illustration of the trajectories of two surface drifters (in red and green) in May 2014 on the northern coast of Mallorca Island. *WMOP_forecast* velocities are represented with blue arrows. Right: trajectories (in grey) of a cluster of 1000 particles advected by the *WMOP_forecast* model surface velocities (the mean trajectory is represented in red, the final positions with red dots), and trajectory of a drifter (in black) during the same t-day period in July 2017, highlighting the importance of daily sea-breezes on the drifter and model-derived trajectories.

High frequency (HF) radar

Using radio waves emitted from fixed antennas on shore, HF radars provide continuous (hourly) real-time coastal surface current mapping, with a limited geographical coverage but a high spatiotemporal resolution. They provide insights into the small-scale variability of coastal ocean currents, knowledge of which is in high demand for practical applications but extremely challenging for operational ocean models. SOCIB operates a 2-CODAR-Sea-Sonde-antenna system, transmitting at 13.5 MHz and monitoring the eastern side of the Ibiza Channel. The spatial resolution is 3 km. Velocity data are delivered hourly and are available in real-time. The area covered by the HF radar extends from the coast to 60 km offshore.

The comparison of the mean velocity fields between model and measurements allows us to detect circulation biases in the model at the coastal scale, which is not properly resolved by altimetry. In the illustration in Fig. 24.18, the model represents an energetic northward vein in the mean circulation in the area covered by the HF radar, overestimating velocities compared to the measurements during this period. This vein is associated with inflows of water of Atlantic origin through the Ibiza Channel. The change of direction of the surface velocities from northwards to southwards observed by the HF radar around 0.9°E is found to be misplaced here in the model with a spatial error around 40 km towards the north-west.

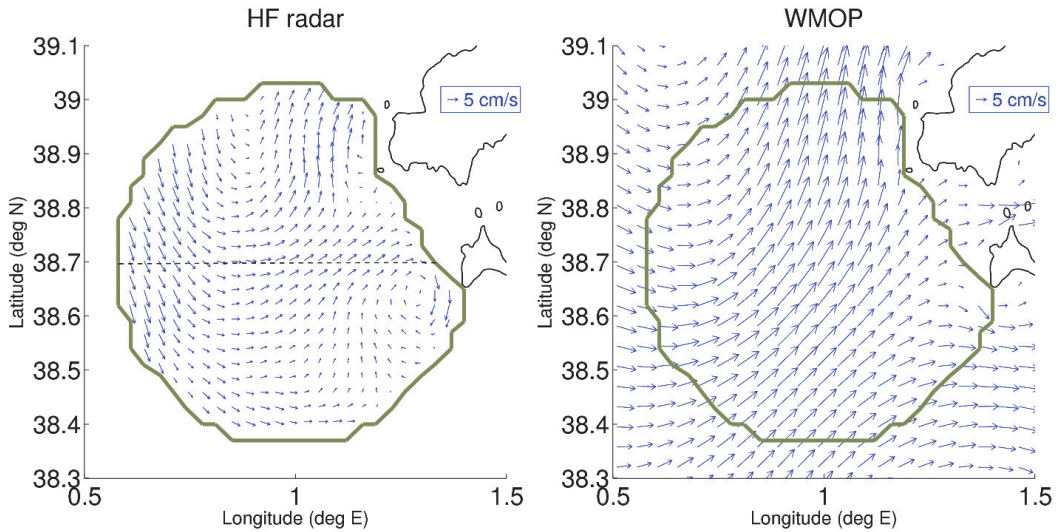


Figure 24.18. Mean surface velocity field from the radar and the *WMOP_hindcast* simulation in the Ibiza Channel over the period 01-June-2012 to 30-Sept-2014. The dashed line at 38.7°N on the left panel shows the position of the section illustrated in Fig. 24.20.

HF radar measurements also provide EKE estimates of the surface ocean at high resolution, which can be compared to models and complement the comparison based on altimetry. Figure 24.19 shows that while EKE have similar magnitudes in the model and in the data in the northern part of the area covered by the HF radar, the model is found to overestimate the eddy activity in the southern part of the region.

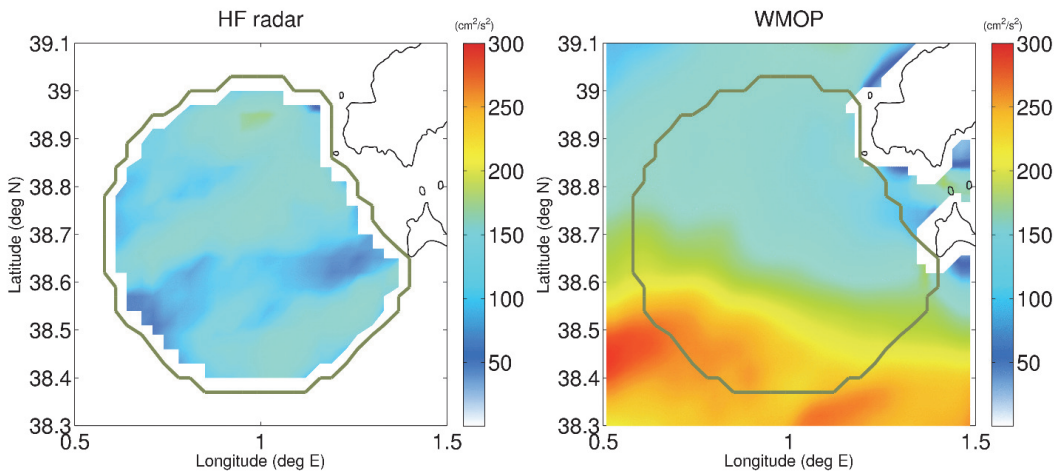


Figure 24.19. Mean EKE estimated from daily mean HF radar data and the *WMOP_hindcast* simulation over the period 01-June-2012 to 30-Sept-2014.

The availability of time series also allows for the assessment of the model capacity to represent sporadic events. Fig. 24.20 shows such a HF radar-model data comparison in the form of a Hovmöller diagram along a zonal section at 38.7°N, considering the *WMOP_hindcast*, the *WMOP_forecast*, the CMEMS-MED model (REAN until 31-Dec-2015, AN-FC afterwards), as well as mapped altimetry. This representation is useful to examine the representation of northwards

and southwards flows through the Ibiza Channel. It reveals the HF variability in the radar and in the different models, which is larger than that provided by interpolated altimetry. Larger velocity standard deviations are found in the model when compared to the radar, especially in the case of the *WMOP_forecast*. The overall pattern correspondence between models and radar is relatively poor, except the strong northward event in July 2016, which is represented in the radar, the *WMOP_forecast*, CMEMS-MED, and also in altimeter data.

Finally, it is worth noting that spatiotemporal HF radar data also allow for the evaluation of the model in terms of EOFs modes, complex correlations, or variability ellipses. Advanced gap-filling methods can be implemented to fill short spatial data gaps in the HF radar data time series (e.g., Lekien et al., 2004; Erick et al., 2016).

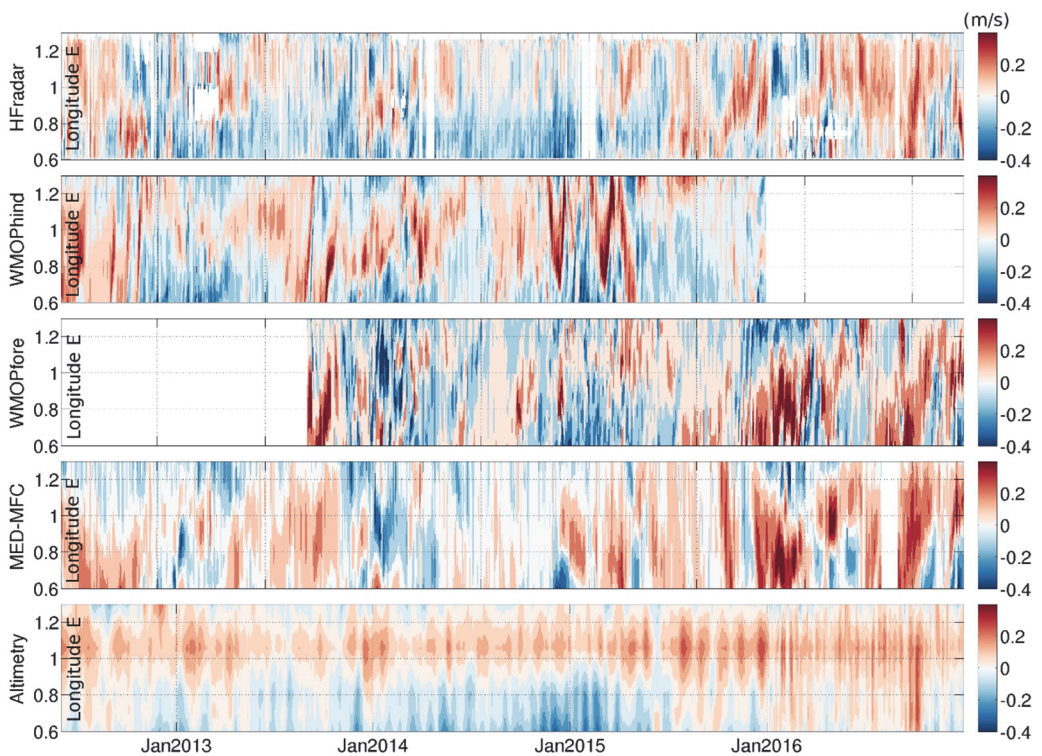


Figure 24.20. Hovmöller diagram of meridional surface velocities (m/s) across the zonal section at 38.7°N shown in Fig. 24.18, from the radar, *WMOP_hindcast*, *WMOP_forecast*, CMEMS-MED model (REAN until 31-Dec-2015, AN-FC afterwards) and altimetry. Red (respectively blue) represents northward (resp. southwards) velocities.

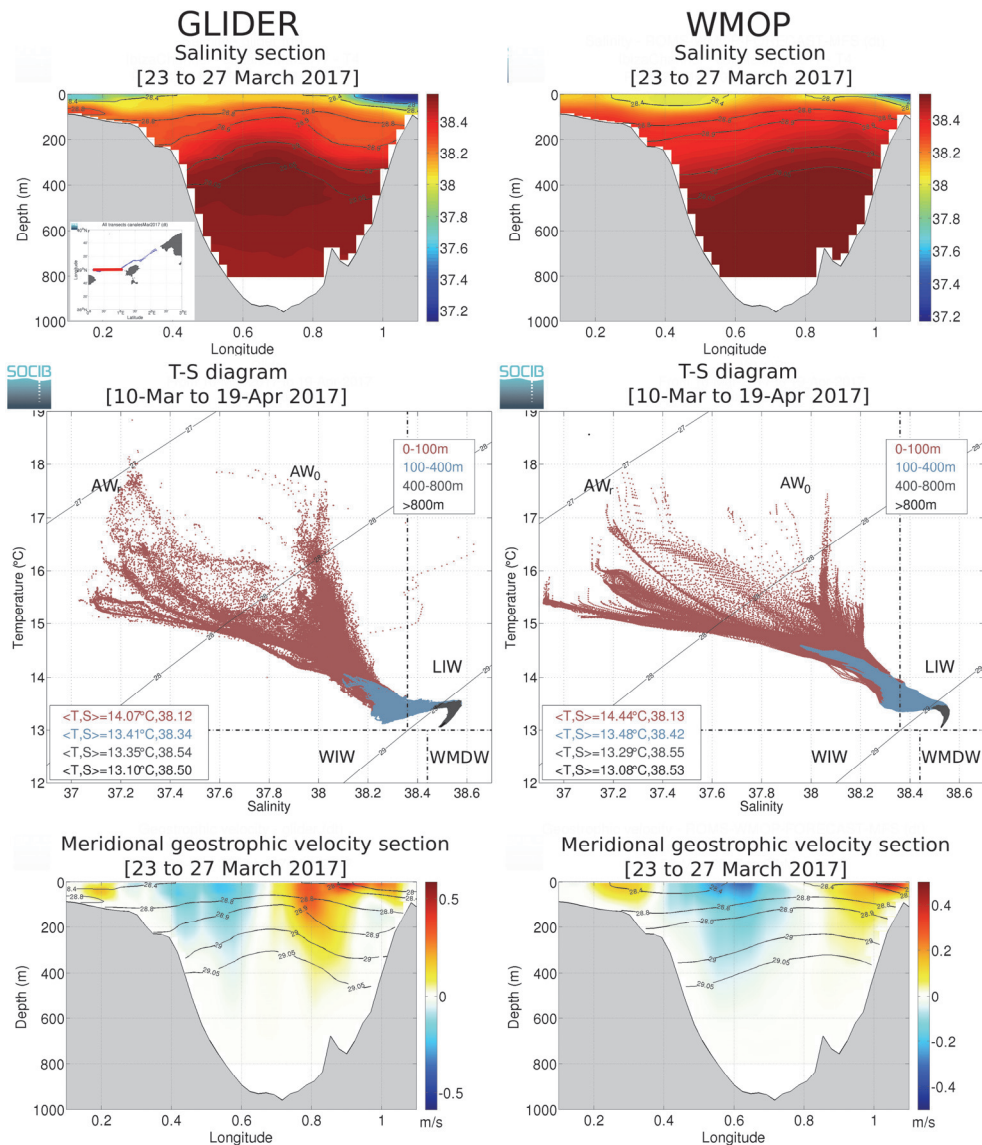


Figure 24.21. Top: vertical salinity section from the glider (left) and the *WMOP* forecast model (right) during the Canales mission in March 2017 (glider tracks are plotted in the insert). Middle: associated T-S diagrams. Bottom: cross-section geostrophic velocities estimated from the glider and model hydrographic sections.

Gliders

Gliders are steerable autonomous vehicles that have the capacity to monitor oceanic sections down to 1000 m depth with high resolution at a forward speed around 20 km per day and transmit data in real time. Typical glider sensors collect data of conductivity, temperature, chlorophyll, and oxygen. The data are unique to detect fine-scale structures in the ocean and to relate the variability of biochemical and physical variables. Gliders are low energy consumers and may be used for missions of several weeks at sea. They are often deployed repetitively along endurance lines, thus providing

time series of hydrographic sections and associated cross-section geostrophic transport variability. Glider data also allow us to distinguish different water masses present along a specific section and then compute the across-section transports of the different water masses. Thanks to their controllability, fleets of gliders can be deployed in a coordinated manner to provide an adaptive sampling of specific targeted ocean circulation features (e.g., Leonard et al., 2010, Alvarez and Mourre, 2014).

SOCIB operates an endurance glider line in the Ibiza Channel in order to monitor meridional water mass exchanges in the Western Mediterranean Sea. The data from the Ibiza Channel glider section (shown in Fig. 24.21) reveals the presence of different water masses: AWo and AWr with significant salinity differences at the surface, and more saline Levantine Intermediate Water at intermediate levels. The model properly represents the presence of AWr on the eastern side of the Ibiza Channel, less accurately on the western side. The subsurface salinity maximum associated with Levantine Intermediate Water is not as marked in the model as it is in the observations, highlighting some model deficiencies in representing this intermediate water mass.

Since 2011, the repetitivity of the glider sections has revealed the high temporal variability of the meridional water mass exchanges through the Ibiza Channel (Heslop et al., 2012). After a few years, the time series has also allowed for the identification of the main modes of variability of temperature, salinity, and cross-section geostrophic velocities, and for the analysis of seasonal and interannual signals in the water mass exchanges, as well as changes in the water mass properties. All of these aspects can be evaluated in the model. Fig. 24.22 illustrates the variability of the transports per water mass for all available Ibiza Channel transects between January 2011 and December 2015. It shows the high transport variability in both the model and the observations. The model generally fails in exactly representing the real transport fluctuations. However, large transports in 2012 are properly described, as well as southward events in 2014 and 2015. The model is also able to form Western Intermediate Water and propagate it until the Ibiza Channel in 2011, 2012, and 2013, as also detected by the glider. No Western Intermediate Water is present in the Ibiza Channel in 2014 and 2015 in model or in observations.

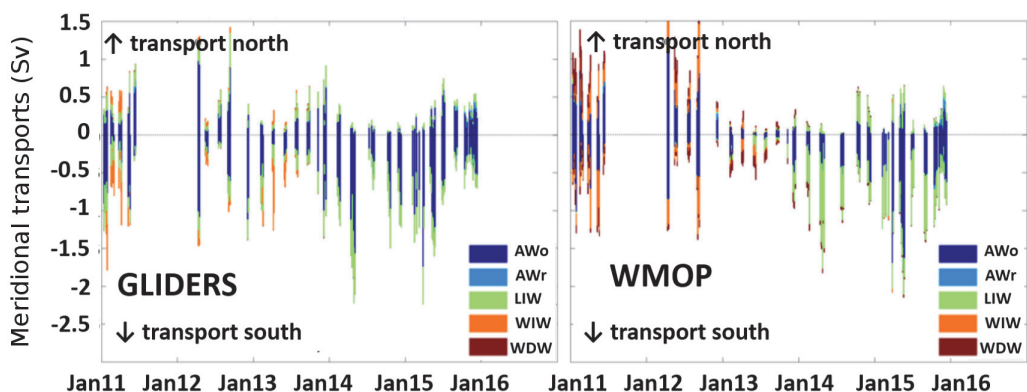


Figure 24.22. Meridional geostrophic transport (Sv) of the different water masses across the Ibiza Channel endurance line as seen by the gliders (left) and the *WMOP* hindcast simulation (right).

Conclusions

Ocean model assessment is a multi-variable, region-dependent, multi-scale problem constrained by available observations and specific user needs requiring specific measures of the model performance. No single metrics can fairly represent the whole performance of a model. In addition, the standard point-wise statistics might penalize high-resolution simulations properly representing ocean structures but misplaced with respect to observations, making necessary the definition of advanced metrics for the quantification of model-data differences.

Multiple platforms collecting measurements of different variables at different scales provide various insights into the model performance. Satellites, Argo floats, fixed moorings, surface drifters, HF radar, and gliders all provide specific and complementary assessments of the models. They allow to evaluate a wide range of different properties, from the large-scale to the fine-scale and coastal variability represented in high-resolution models. The following oceanographic features have been illustrated in this chapter:

- the mean large-scale surface circulation
- the associated EKE and modes of variability
- the presence and propagation of eddies
- the spatial and temporal variability of the SST
- the vertical stratification and the depth of the mixed layer
- the vertical modes of variability of ocean currents at a fixed location
- the representation of specific coastal circulation processes (coastal gyre, sea breeze effects)
- the coastal surface circulation, EKE, and representation of inflow events in the Ibiza Channel
- the representation of surface and intermediate water masses in the Ibiza Channel and their corresponding meridional transport

These multi-platform data allow us to evaluate the realism of the model both in terms of statistical behaviour and representation of sporadic events. The following references are highly recommended for the reader interested in more detailed quantitative multi-platform ocean regional model assessment exercises (Oke et al., 2002; Warner et al., 2005; Penduff et al., 2006; Chiggiato and Oddo, 2008; Chao et al., 2009; Liu et al., 2009; Wilkin and Hunter, 2013; Lorente et al., 2014; Juza et al., 2015; Capó et al., 2016).

The integration of this multiple information into synthetic metrics addressing specific user needs now constitutes an important challenge in operational oceanography. The application of neighborhood validation methods, probabilistic approaches, advanced Lagrangian diagnostics, front detection algorithms from high-resolution satellite imagery, and the analysis of high-resolution altimetry certainly also represent important future directions for the evaluation of high-resolution ocean simulations.

Acknowledgements

We are very grateful for the helpful comments on the manuscript by the students of the GODAE OceanView Summer School, Hanna Kauko, Christina Kong and Jean-Baptiste Kassi, as well as the anonymous reviewer. The WMOP hindcast simulation and corresponding assessment has been developed in the framework of the MEDCLIC project funded by La Caixa Foundation. Validation using coastal platforms is part of the H2020 JERICO-NEXT project. Eddy tracker outputs have been obtained during the MEDSUB project funded by the CMEMS Service Evolution Programme. We gratefully acknowledge Puertos del Estado for making data available from their mooring network, AEMET for providing HIRLAM atmospheric fields, and CMEMS for the large-scale Mediterranean model products.

References

- Alvarez A. and B. Mourre (2014). Cooperation or coordination of underwater glider networks? An assessment from Observing System Simulation Experiments in the Ligurian Sea. *J. Atmos. And Ocean. Technology*, 31, 2268-2277.
- Belkin I.M. and J.E. O'Reilly (2009). An algorithm for oceanic front detection in chlorophyll and SST satellite imagery. *Journal of Marine Systems*, 78, 319-326.
- Buongiorno Nardelli B., C. Tronconi, A. Pisano, R. Santoleri, (2013). High and Ultra-High resolution processing of satellite Sea Surface Temperature data over Southern European Seas in the framework of MyOcean project. *Rem. Sens. Env.*, 129, 1-16, doi:10.1016/j.rse.2012.10.012
- Capó E., A.Orfila, Sayol J.-M., Conti D., Juza, M., Ruiz S., Sotillo M.G., García-Ladona E., Simarro G., Mourre B. and Tintoré J. (2016). Assessment of operational models in the Balearic Sea during the MEDESS experiment. *Deep Sea Research*, 133, 118-131, doi:10.1016/j.dsr.2016.03.009.
- Chao Y, Li Z, Farrara J, McWilliams C, Bellingham J, Capet X, Chavez F, Choi J-K, Davis R, Doyle J, et al. (2009). Development, implementation and evaluation of a data-assimilative ocean forecasting system off the central California coast. *Deep-Sea Res II*. 56: 100–126.
- Candille G. and O. Talagrand (2005). Evaluation of probabilistic prediction systems for a scalar variable. *Q.J.R. Meteorol. Soc.* , 131, pp. 2131-2150.
- Casati, B. et al., (2008). Forecast verification: Current status and future directions. *Meteor. Appl.*, 15, 3–18.
- Chelton, D. B., M. G. Schlax, and R. M. Samelson (2011). Global observations of nonlinear mesoscale eddies, *Prog. Oceanogr.*, 91, 167–216, doi:10.1016/j.pocean.2011.01.002.
- Chiggiato J, Oddo P. (2008). Operational ocean models in the Adriatic Sea: a skill assessment. *Ocean Sci.* 4:61–71.
- Clementi E., Pistoia J., Fratianni C., Delrosso D., Grandi A., Drudi M., Coppini G., Lecci R., Pinardi N. (2017). “Mediterranean Sea Analysis and Forecast (CMEMS MED-Currents 2013-2017)”. [Data set]. Copernicus Monitoring Environment Marine Service (CMEMS). doi:10.25423/MEDSEA_ANALYSIS_FORECAST_PHYS_006_001
- Davis, R. E. (1985). Drifter observations of coastal surface currents during CODE: The method and descriptive view, *J. Geophys. Res.*, 90, 4741-4755, doi:10.1029/JC090iC03p04741.
- Ebert, E.E., (2009). Neighborhood Verification: A Strategy for Rewarding Close Forecasts. *Wea. Forecasting*, 24, 1498–1510, doi:10.1175/2009WAF2222251.1
- Emery, W. J. and Thompson, R. E. (2001). *Data analysis methods in physical oceanography*. Elsevier, Oxford, UK
- Erick, F., Hugh, R., Josh, K., Michael, S., Scott, G. (2016). Gap Filling of the Coastal Ocean Surface Currents from HFR Data: Application to the Mid-Atlantic Bight HFR Network. *Journal of Atmospheric and Oceanic Technology* 33, 1097-1111.
- Escudier, R., L. Renault, A. Pascual, P. Brasseur, D. Chelton, and J. Beuvier (2016a). Eddy properties in the Western Mediterranean Sea from satellite altimetry and a numerical simulation, *J. Geophys. Res. Oceans*, 121, 3990–4006, doi:10.1002/2015JC011371.
- Escudier, R., B. Mourre, M. Juza, and J. Tintore (2016b). Subsurface circulation and mesoscale variability in the Algerian subbasin from altimeter-derived eddy trajectories, *J. Geophys. Res. Oceans*, 121, 6310–6322, doi:10.1002/2016JC011760.

- Halo, I., B. Backeberg, P. Penven, I. Ansonge, C. Reason, and J. Ullgren (2013). Eddy properties in the Mozambique Channel: A comparison between observations and two numerical ocean circulation models, *Deep Sea Res., Part II*, 100, 38–53.
- Hernandez F., E. Blockley, G. B. Brassington, F. Davidson, P. Divakaran, M. Drévillon, S. Ishizaki, M. Garcia-Sotillo, P. J. Hogan, P. Lagema, B. Levier, M. Martin, A. Mehra, C. Mooers, N. Ferry, A. Ryan, C. Regnier, A. Sellar, G. C. Smith, S. Sofianos, T. Spindler, G. Volpe, J. Wilkin, E. D. Zaron and A. Zhang (2015). Recent progress in performance evaluations and near real-time assessment of operational ocean products, *Journal of Operational Oceanography*, 8:2, s221-s238, doi: 10.1080/1755876X.2015.1050282.
- Heslop, E.E., Ruiz, S., Allen, J., López-Jurado, J.L., Renault, L., Tintoré, J. (2012). Autonomous underwater gliders monitoring variability at “choke points” in our ocean system: A case study in the Western Mediterranean Sea. *Geophysical Research Letters*, 39.
- Isern-Fontanet, J., García-Ladona, E., Font, J., (2003). Identification of marine eddies from altimetry. *Journal of Atmospheric and Oceanic Technology* 20, 772-778.
- Jolliff JK, Kindle JC, Shulman I, Penta B, Friedrichs MAM, Helber R, Arnone R (2009). Summary diagrams for coupled hydrodynamic-ecosystems model skill assessment. *J Mar Syst*, 76, 64–82
- Juza, M., Mourre, B., Lellouche, J.-M., Tonani, M., and Tintoré, J. (2015). From basin to sub-basin scale assessment and intercomparison of numerical simulations in the western Mediterranean Sea. *Journal of Marine System*, 149, 36-49, doi:10.1016/j.jmarsys.2015.04.010.
- Juza, M., Mourre, B., Renault, L., Gómar, S., Sebastián, K., Lora, S., Beltran, J.P., Frontera, B., Garau, B., Troupin, C., Torner, M., Heslop, E., Casas, B., Escudier, R., Vizoso, G., Tintoré, J. (2016). SOCIB operational ocean forecasting system and multi-platform validation in the Western Mediterranean Sea. *Journal of Operational Oceanography*, 9, s155-s166.
- Kerry C., B. Powell, M. Roughan and P. Oke (2016). Development and evaluation of a high-resolution reanalysis of the East Australia Current region using the Regional Ocean Modelling System (ROMS3.4) and Incremental Strong-Constraint 4-Dimensional Variational (IS4D-Var) data assimilation. *Geoscientific Model Development*, 9(10), pp. 3779-3801.
- Kourafalou VH, De Mey P, Le Hénaff M, Charria G, Edwards CA, He R, Herzfeld M, Pasqual A, Stanev E, Tintoré J, Usui N, Van Der Westhuysen A, Wilkin J, Zhu X. (2015). Coastal Ocean Forecasting: system integration and validation. *J Oper. Oceanogr.* 8(1).
- Kurapov. A., S. Erofeeva and E. Myers (2017). Coastal sea level variability in the US West Coast Ocean Forecast System (WCOFS). *Ocean Dynamics*, 67, 23-36.
- Lekien, F., Coulliette, C., Bank, R., Marsden, J. (2004). Open-boundary modal analysis: Interpolation, extrapolation, and filtering. *Journal of Geophysical Research: Oceans* 109, C12004.
- Leonard N.E., D. Paley, R. Davis, D. Fratantoni, F. Lekien and F. Zhang (2010). Coordinated control of an underwater glider fleet in an adaptive sampling field experiment in Monterey Bay. *J. Field Robotics*, 27, 718-740.
- Liu, Y., and R. H. Weisberg (2011). Evaluation of trajectory modeling in different dynamic regions using normalized cumulative Lagrangian separation, *J. Geophys. Res.*, 116, C09013, doi:10.1029/2010JC006837.
- Le Traon, P. Y., P. Klein, B. L. Hua, and G. Dibarboure (2008). Do altimeter wavenumber spectra agree with the interior or surface quasigeostrophic theory?, *J. Phys. Oceanogr.*, 38, 1137-1142, doi:10.1175/2007JPO3806.1.
- Liu, Y., P. MacCready, B. M. Hickey, E. P. Dever, P. M. Kosro, and N. S. Banas (2009). Evaluation of a coastal ocean circulation model for the Columbia River plume in summer 2004, *J. Geophys. Res.*, 114, C00B04, doi:10.1029/2008JC004929.
- Lorente P., S. Piedracoba, M. García Sotillo, R. Aznar, A. Amo-Baladrón, A. Pascual, J. Soto-Navarro and E. Álvarez-Fanjul (2016). Ocean model skill assessment in the NW Mediterranean using multi-sensor data, *Journal of Operational Oceanography*, 9:2, 75-92, doi:10.1080/1755876X.2016.1215224
- Marchesiello P, McWilliams JC, Shchepetkin A. (2001). Open boundary conditions for long-term integration of regional oceanic models. *Ocean Modell.* 3:1–20.
- Mason, E., A. Pascual, and J.C. McWilliams (2014). A New Sea Surface Height–Based Code for Oceanic Mesoscale Eddy Tracking. *J. Atmos. Oceanic Technol.*, 31, 1181–1188, doi:10.1175/JTECH-D-14-00019.1.
- Millot, C. (1985). Some features of the Algerian current. *Journal of Geophysical Research* 90 (C4), 7169–7176.
- Millot, C. (1999). Circulation in the western Mediterranean Sea, *J. Mar. Syst.*, 20(1-4), 423–442, doi:10.1016/S0924-7963(98)00078-5.

- Millot C. and I. Taupier-Letage (2005). Circulation in the Mediterranean Sea. *Handbook of Environmental Chemistry*, Vol. 5, Part K: 29–66, doi:10.1007/b107143
- Mittermaier and Csima (2017). Ensemble versus Deterministic Performance at the Kilometer scale. *Weather and Forecasting*, 32, 1697-1709.
- Murphy AH (1995). The coefficients of correlation and determination as measures of performance in forecast verification. *Wea. Forecasting*, 10, 681-688.
- Nencioli, F., C. Dong, T. Dickey, L. Washburn, and J. C. McWilliams (2010). A vector geometry-based eddy detection algorithm and its application to a high-resolution numerical model product and high-frequency radar surface velocities in the southern California bight, *J. Atmos. Oceanic Technol.*, 27(3), 564–579.
- Nittis K, Zervakis V, Perivoliotis L, Papadopoulos A, Chronis G. (2001). Operational monitoring and forecasting in the Aegean Sea: system limitations and forecasting skill evaluation. *Marine Pollut Bull.* 43: 154–163.
- Oke, P. R., J. S. Allen, R. N. Miller, G. D. Egbert, J. A. Austin, J. A. Barth, T. J. Boyd, P. M. Kosro, and M. D. Levine (2002). A modeling study of the three-dimensional continental shelf circulation off Oregon. Part I: Model-data comparisons, *J. Phys. Oceanogr.*, 32, 1360–1382.
- Okubo, A. (1970). Horizontal dispersion of floatable particles in the vicinity of velocity singularities such as convergences. *Deep-Sea Res.*, 17, 445–454.
- Oreskes, N., Shrader-Frechette, K., Belitz, K. (1994). Verification, validation and confirmation of numerical models in the earth sciences. *Science* 263 (5147), 641–646.
- Pascual, A., E. Vidal-Vijande, S. Ruiz, S. Somot and V. Papadopoulos (2014). Spatiotemporal variability of the surface circulation in the Western Mediterranean: a comparative study using altimetry and modeling. In: *The Mediterranean Sea: Temporal variability and spatial patterns*, John Wiley & Sons, Inc., doi:10.1002/9781118847572.ch2
- Peacock T. and G. Haller (2013). Lagrangian coherent structures: the hidden skeleton of fluid flows. *Phys. Today*, 66(2), 41.
- Penduff, T., B. Barnier, J.-M. Molines, and G. Madec. (2006). On the use of current meter data to assess the realism of ocean model simulations, *Ocean Modelling*, 11, 3-4, 399-416.
- Rio, M.-H., A. Pascual, P.-M. Poulain, M. Menna, B. Barcelo, and J. Tintore (2014). Computation of a new mean dynamic topography for the Mediterranean Sea from model outputs, altimeter measurements and oceanographic in-situ data, *Ocean Sci. Discuss.*, 11(1), 655–692.
- Robinson, A. R., W. G. Leslie, A. Theocharis, and A. Lascaratos (2001). *Mediterranean Sea circulation, Ocean Currents: A Derivative of the Encyclopedia of Ocean Sciences*, Academic Press, pp. 1689–1705.
- Sakamoto K., G. Yamanaka, H. Tsujino, H. Nakano, S. Urakawa, N. Usui, M. Hirabara and K. Ogawa (2016). Development of an operational coastal model of the Seta Inland Sea, Japan, *Ocean Dynamics*, 66 (1), pp. 77-97.
- Sandvik A.D., Ø. Skagseth, M. D. Skogen (2016). Model validation: Issues regarding comparisons of point measurements and high-resolution modeling results, *Ocean Modelling*, 106, 68-73.
- Shchepetkin, A.F., McWilliams, J.C. (2005). The regional oceanic modeling system (ROMS): a split-explicit, free-surface, topography-following-coordinate oceanic model. *Ocean Modelling*, 9, 347-404.
- Siddorn JR, Allen JI, Blackford JC, Gilbert FJ, Holt JT, Holt MW, Osborne JP, Proctor R, Mills DK. (2007). Modelling the hydro-dynamics and ecosystem of the North-west European Continental Shelf for operational oceanography. *J Mar Syst* 65: 417–429.
- Simoncelli, S., Fratianni, C., Pinardi, N., Grandi, A., Drudi, M., Oddo, P., and Dobricic, S. (2014). "Mediterranean Sea physical reanalysis (MEDREA 1987-2015)". [Data set]. EU Copernicus Marine Service Information. DOI: https://doi.org/10.25423/medsea_reanalysis_phys_006_004
- Stanev E, Schulz-Stellenfleth J, Staneva J, Grayek S, Seemann J, Petersen W. (2011). Coastal observing and forecasting system for the German Bight. Estimates of hydro-physical states. *Ocean Sci.* 7: 1–15.
- Taylor KE (2001). Summarizing multiple aspects of model performance in a single diagram. *J Geophys Res*, 106, 7183–7192
- Tintoré, J., et al. (2013). SOCIB: The Balearic Islands Coastal Ocean Observing and Forecasting System Responding to Science, Technology and Society Needs. *Marine Technology Society Journal*, 47, 101-117.
- Undén, P., et al. (2002). The HIRLAM version 5.0 model. *HIRLAM documentation manual (HIRLAM Scientific Documentation)*. Available at <http://www.knmi.nl/hirlam/SciDocDec2002.pdf> or from Hirlam-5 Project, SMHI, S-60176, Norrköping, Sweden.
- Umlauf, L., Burchard, H. (2003). A generic length-scale equation for geophysical turbulence models. *J. Marine Res.* 61,235–265.
- Warner, J. C., W. R. Geyer, and J. A. Lerczak (2005). Numerical modeling of an estuary: A comprehensive skill assessment, *J. Geophys. Res.*, 110, C05001, doi:10.1029/2004JC002691.

- Weiss, J. (1991). The dynamics of enstrophy transfer in two-dimensional hydrodynamics. *Physica D*, 48, 273–294.
- Wilkin J. L., H.G. Arango, D.B. Haidvogel, C.S. Lichtenwalner, S.M. Glenn and K. S. Hedström (2005). A regional ocean modelling system for the Long-term Ecosystem Observatory, *J. Geophys. Res.*, 110, C06S91, doi:10.1029/2003JC002218.
- Wilkin, J. L., and E. J. Hunter (2013). An assessment of the skill of real-time models of Mid-Atlantic Bight continental shelf circulation, *J. Geophys. Res. Oceans*, 118, 2919–2933, doi:10.1002/jgrc.20223.
- Willmott, C. J. (1981). On the validation of models, *Phys. Geogr.*, 2, 184–194.
- Ziegeler S., Dykes J. and J. Shriver (2012). Spatial error metrics for oceanographic model verification. *J. Atmos. Oceanic Technol.*, 29, 260-266.

